Am J Cancer Res 2020;10(11):3973-3989
www.ajcr.us /ISSN:2156-6976/ajcr0120083

Original Article

Clonal expansion of bone marrow CD8$^+$ T cells in acute myeloid leukemia patients at new diagnosis and after chemotherapy

Zhongxin Feng[1,2,3], Qin Fang[4], Xingyi Kuang[1,2,3], Xin Liu[1,2,3], Ying Chen[2,3], Dan Ma[2,3], Jishi Wang[1,2,3]

[1]Department of Clinical Medical School, Guizhou Medical University, Guiyang, Guizhou, China; [2]Department of Hematology, Affiliated Hospital of Guizhou Medical University, Guiyang, Guizhou, China; [3]Department of Guizhou Province Hematopoietic Stem Cell Transplantation Center and Key Laboratory of Hematological Disease Diagnostic and Treatment Centre, Guiyang, Guizhou, China; [4]Department of Pharmacy, Affiliated Hospital of Guizhou Medical University, Guiyang, Guizhou, China

Received August 11, 2020; Accepted October 20, 2020; Epub November 1, 2020; Published November 15, 2020

Abstract: CD8$^+$ T cells are crucial adaptive immune effectors and express receptors (T cell receptors, TCRs) that specifically recognize and eradicate tumor cells. The diversity of the TCR repertoire is generated by specialized genetic diversification mechanisms, which lead to an extremely variable TCR repertoire that is capable of recognizing a wide range of antigens. However, the variations in CD8$^+$ TCR diversity and their clinical implications in acute myeloid leukemia (AML) patients remain unknown. CD8$^+$ T cells were enriched from 10 healthy donors and 31 AML patients at diagnosis and after chemotherapy, and TCRβ deep sequencing was performed to analyze CD8$^+$ T cell clonal expansion and TCR repertoire diversity. Diminished TCR repertoire diversity and increased T cell clone expansion were noted in the bone marrow of AML patients. In relapsed patients, T cells were found to be more clonally expanded after chemotherapy than at new diagnosis. Moreover, significantly more expanded TCRβ clonotypes were noted in CD8$^+$ PD-1$^+$ T cells than in CD8$^+$ PD-1$^-$ T cells regardless of the time of examination. Our systematic T cell repertoire analysis may help better characterize CD8$^+$ T cells before and after chemotherapy in AML, which may provide insights into therapeutic strategies for hematological malignancies.

Keywords: CD8$^+$ T cell, T cell receptor, bone marrow, programmed death-1, acute myeloid leukemia

Introduction

Acute myeloid leukemia (AML) is a progressive malignant disorder that is often associated with poor survival rates. In recent decades, little has changed in the induction chemotherapy used to treat AML. While the majority of AML patients achieve complete remission (CR) at the outset, most of them fail to sustain such responses for a long time due to chemoresistance [1]. Considerable effort has been dedicated to elucidating the drug resistance mechanisms in leukemia, but little attention has been paid to the differences in immune signaling in response to chemotherapy between responsive patients and nonresponsive patients [2]. Cancer immunotherapy has attracted considerable attention as a novel therapeutic approach because of reported successes in checkpoint blockade intervention and T cell engineering [3]. Potential new immunotherapeutic modalities hold much promise for the treatment of AML and are likely to increase in the future [4-8]; however, many significant challenges remain [9, 10]. Hence, characterization of the immune and biological features of this disease is the key to optimizing the therapeutic strategy for AML patients.

CD8$^+$ T cells are the main cytotoxic effector cells and mediate apoptosis through the T cell receptor (TCR), which recognizes tumor-expressed antigenic peptides bound to MHC class I molecules [11]. The TCR is composed of two constituent chains (αβ or γδ), which undergo a V(D)J recombination process. As the most diverse portion of the variable region, complementarity-determining region 3 (CDR3) is the

primary contributor to the specificity of T cell antigen recognition [12, 13]. Recent studies suggested that δ-CDR3s in γδ T cells can predict clinical responses in AML patients [14, 15]. Despite the potential of the TCR as a therapeutic target, $CD8^+$ TCR repertoire dynamics and the mechanisms by which the TCR is modulated during chemotherapy are still poorly understood. αβ T cells are the predominant subset, making up approximately 90-95% of all peripheral T cells in healthy adults [16]. Therefore, it is crucial to assess the characteristics of the $CD8^+$ TCR repertoire and investigate its clinical significance in AML patients.

It has become increasingly clear that programmed death-1 (PD-1) is a key regulator of T cell dysfunction after exposure to antigen stimulation [17]. A recent study reported functional skewing of $CD8^+$ T cells in newly diagnosed AML patients, which was correlated with upregulation of PD-1 expression [18]. As expected, the response to chemotherapy is associated with upregulation of costimulatory molecules and attenuation of apoptotic signaling [19]. Compared to that at the time of new diagnosis, significantly higher PD-1 expression on $CD8^+$ T cells was noted at the time of relapse. However, treatment with PD-1 pathway blockade or the costimulatory molecule OX40 results in increased $CD8^+$ T cell effector function [2, 6, 20]. These findings indicated that implicated $PD\text{-}1^+$ $CD8^+$ T cells in AML progression and suggested that this factor may be used to promote cytotoxicity.

The diversity of the TCR repertoire may reflect differential recognition of neoantigens. The $PD\text{-}1^+$ $CD8^+$ phenotype has been identified as a marker of T cell exhaustion and has been proven to display neoantigen-specific cytotoxic activity [21, 22]. A diversified TCR repertoire enables the host immune system to recognize a large variety of tumor neoantigens [23]. Hence, an improved understanding of the $PD\text{-}1^+$ $CD8^+$ TCR repertoire would enable more effective clinical and therapeutic strategies for AML patients.

In this study, we performed RNA sequencing of the CDR3 region from TCRβ chains of αβ $CD8^+$ T cells and examined the different clonal expansion patterns between AML and healthy donor samples. In addition, we analyzed T cell clonality and distribution in paired patient samples collected at diagnosis and after chemotherapy. We further studied the TCR repertoire dynamics of $PD\text{-}1^-$ negative and $PD\text{-}1^-$ positive $CD8^+$ T cells. We found that TCR repertoire diversity was correlated with clinical outcomes. Collectively, these results underscored the antitumor reactivity of $CD8^+$ T cells and the value of the $CD8^+$ T cell repertoire as a potential prognostic marker for AML, highlighting the importance of immune intervention.

Materials and methods

Samples

This study was approved by the Institutional Review Board (IRB) of the Affiliated Hospital of Guizhou Medical University. All subjects provided their written informed consent in accordance with the Declaration of Helsinki. The clinical and demographic data for all the subjects are summarized in Table S1. Peripheral blood mononuclear cells (PBMCs) and bone marrow mononuclear cells (BMMCs) were obtained from healthy donors and AML patients at diagnosis and after chemotherapy. Complete remission (CR) was considered to be less than 5% blasts in the bone marrow (BM) by morphologic evaluation, with a neutrophil count greater than 1×10^9/L and a platelet count greater than 1×10^{11}/L.

Flow cytometry

PBMCs or BMMCs were collected via density gradient centrifugation using Ficoll-Paque reagents (GE Healthcare, Sweden), cryopreserved in 90% human serum, and formulated with 10% DMSO. $CD8^+$ T cells were purified using the Dynabeads CD8 Positive Isolation Kit (Life Technologies, Norway) according to the manufacturer's protocol. The purity of sorted T cell samples was >90%, as determined by flow cytometry. PD-1 expression analysis of $CD8^+$ T cells and $CD8^+$ $PD\text{-}1^+$ and $CD8^+$ $PD\text{-}1^-$ T cell sorting was performed on a BD Biosciences FACS Aria II.

RNA isolation and TCRβ sequencing

$CD8^+$ T cells were enriched using the Dynabeads CD8 Positive Isolation Kit. RNA was extracted using the Ultrapure RNA Kit (Cwbiotech, Beijing, China). For quantitating RNA samples, a Qubit RNA HS Assay Kit (Thermo Fisher Scientific,

Pleasanton CA, USA) was used. The Agilent RNA 6000 Nano Kit and Agilent 2100 Bioanalyzer were used for RNA integrity assessment. For each sample, 20 ng of total RNA was reverse transcribed using SuperScript IV VILO Master Mix (Thermo Fisher Scientific), and then 25 ng cDNA was target amplified using the Oncomine TCR Beta-LR Assay Kit (Thermo Fisher Scientific). Libraries were purified, diluted 1:100 and quantified using the Ion Library Quantitation Kit (Thermo Fisher Scientific) and then diluted to 25 pM with low TE buffer. Samples were pooled on an Ion 530 chip for sequencing via the Ion S5 System, followed by analysis via the Ion Reporter. Total RNA from the Jurkat cell line was obtained from a clonotype with a T cell phenotype. T cell leukemia (Jurkat) total RNA was derived from a cell line consisting of a single T cell clonotype. For the control, running the Oncomine™ TCR Beta Assay on Jurkat total RNA detected a single clonotype.

Equal numbers of available cells in $CD8^+$ $PD\text{-}1^+$ (2~5 × 10^4 cells) and $CD8^+$ $PD\text{-}1^-$ (2~5 × 10^4 cells) T cell populations from each sample were collected for RNA extraction and subsequent TCRβ sequencing.

Data processing and analysis

Repertoire quality metric analysis was performed via the Oncomine™ TCR Beta-LR Assay workflow in the Ion Reporter™ Software. The Shannon index and Gini index were used to characterize the frequency and sequence features of clonotypes. The Gini index was calculated as $\frac{A}{A+B}$, in which, for a set of clone frequencies, A represents the difference between the total area under the line of equality and the area under the Lorenz curve, and B represents the area under the Lorenz curve. The index ranges from 0 to 1. Higher values indicate dissimilar clone sizes, while lower values indicate more similar clone sizes. Shannon entropy was calculated as $-\sum_{i=1}^{R} p_i \log_2(p_i)$, where p_i indicates the frequency of the ith clone, and R indicates the total number of clones [24]. Samples with many clones of similar frequencies have high Shannon diversity. Subsequent analysis of the TCR repertoire was performed using VDJtools [25], tcRpackages [26], Treemap [27], and mothur [28].

The Mann-Whitney U-test was used to determine whether there were differences between the two groups. Analysis of covariance was initially used for the multiple group comparison. Correction for multiple tests was performed using the false discovery rate method. The Wilcoxon signed-rank test was used for matched paired comparisons.

Results

Extensive clonally expanded $CD8^+$ T cell populations in the BM of AML patients

The overall design of this study is shown schematically in **Figure 1**. The distribution plot of the top 100 TCR clonotypes in BM and PB from one AML patient and one healthy donor is shown in **Figure 2A**. The graph demonstrates increased clonal expansion in the BM of the AML patient compared to the other groups. **Figure 2B** shows that the total/unique clonotype ratios were higher in the BM of AML patients than in the PB of AML patients and in the BM and PB of healthy donors. A markedly higher frequency of highly expanded clones (HECs) [29] was noted in the BM and PB of AML patients than in those of healthy donors (**Figure 2C**). In addition, the Shannon index and Gini index were used to evaluate the TCR repertoire diversity. As shown in **Figure 2D**, the Shannon index for the BM of AML patients was significantly higher than that for the PB of AML patients and the BM and PB of healthy donors; in contrast, the Gini index for the BM of AML patients showed a pronounced reduction compared with that for the other groups (**Figure 2E**). Collectively, these findings showed that in $CD8^+$ T cells from the BM of AML patients, a decline in T cell repertoire diversity is closely associated with clonotypic expansion.

Comparison of overall usage of TCRβ V-J rearrangements in AML patients and healthy donors

We identified a total of 60 distinguishable gene transcription segments from the TCRβ V (TRBV) loci, 2 from the TCRβ D (TRBD) loci, 13 from the TCRβ J (TRBJ) loci, and 780 rearrangements in the TRBV-J region. In the graph in **Figure 3A**, each rearrangement event in TRBV-J is denoted by a dot, with its size indicating the average frequency of the rearrangement in the sample group. Similar overall usage profiles of the rearranged TRBV/J segments were noted between BM and PB from healthy donors (81 differentially expressed rearrangements) and

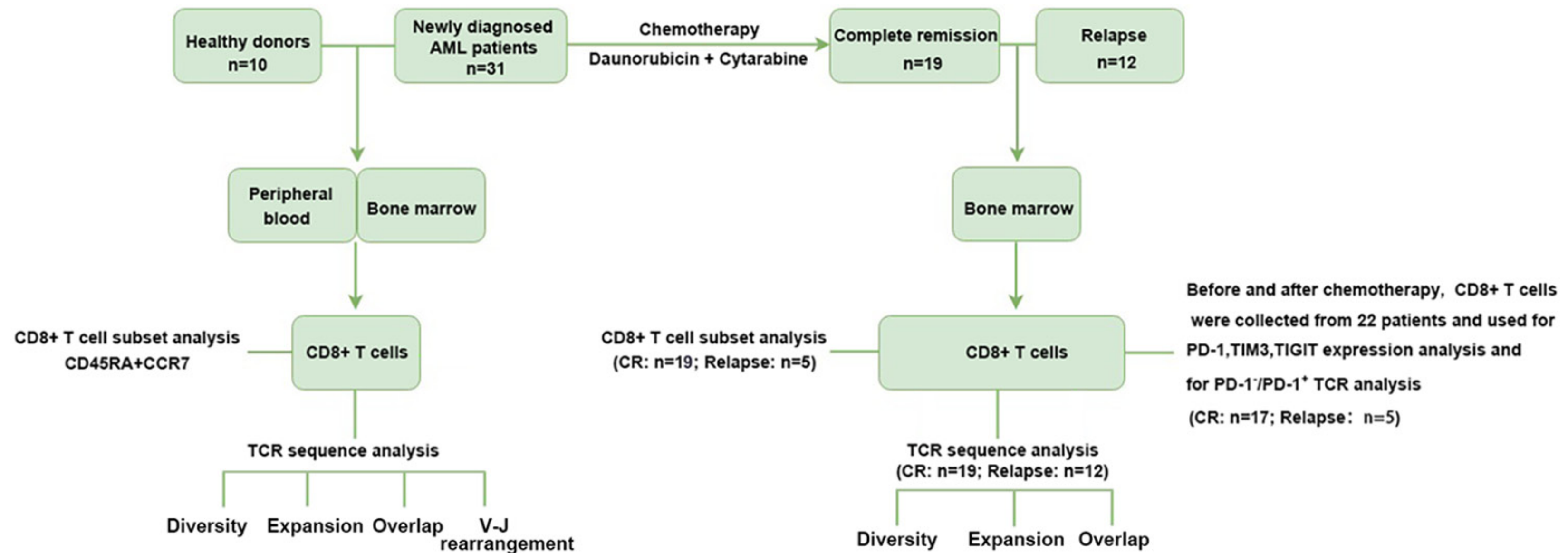

Figure 1. Schematic illustration of the overall study design. The differences of TCR repertoire between AML patients and healthy donors were compared on BM and PB samples by evaluating several indicators, e.g., the CDR3β diversity, V-J usage, clonal expansion and sequence overlap. $CD8^+$ T cells in BM and PB from AML patients and healthy donors were phenotypically analyzed based on the coordinated expression of CD45RA and CCR7. The dynamics of TCR repertoire, phenotypic composition, expression levels of co-inhibitory receptors including PD-1, TIM3, TIGIT, and TCR repertoire distribution in $PD\text{-}1^-$/$PD\text{-}1^+$ T cells were assessed in BM $CD8^+$ T cells from AML patients before and after chemotherapy.

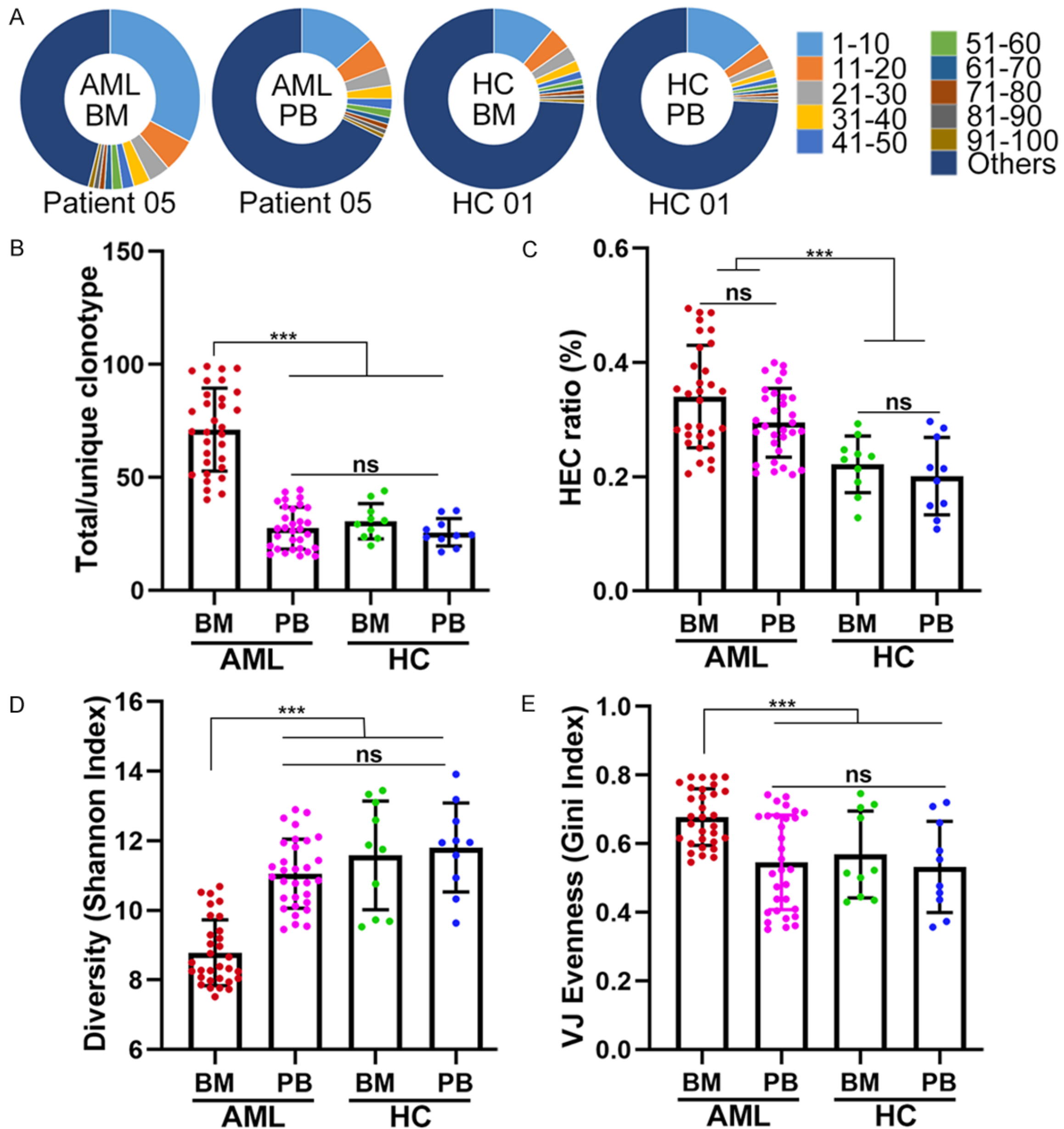

Figure 2. Clonal expansion and diversity of PB and BM CD8+ T cells from AML patients and healthy donors. (A) The distribution profile of the top 100 clonotypes from the BM and PB of one AML patient and one healthy donor, as depicted in a pie chart. The TCR repertoire diversity was evaluated by the total/unique clonotype ratio (B), the HEC ratio (C), the Shannon diversity index (D), and the Gini index (E) in four study groups containing BM (n = 31) and PB (n = 31) samples obtained from AML patients and BM (n = 10) and PB (n = 10) samples obtained from healthy donors. A dot is used to represent one patient or one donor sample. Analysis of covariance was initially used for the multiple group comparison. Correction for multiple tests was performed using the false discovery rate method. ns indicates not significant; *** indicates P < 0.01.

between PB from AML patients and PB from healthy donors (62 differentially expressed rearrangements); however, the differences were greater between BM and PB from AML patients (176 differentially expressed rearrangements) and between BM from AML patients and BM from healthy donors (202 differentially expressed rearrangements) (**Figure 3B-E**). Similarly, we found comparable usage patterns of TRBV gene segments between PB from healthy donors and BM from healthy donors and between PB from healthy donors and PB from

A

Frequency
0.001
0.01
0.05
0.1
0.5
1.0
2.0
5.0

AML-BM

AML-PB

Health-BM

Health-PB

B

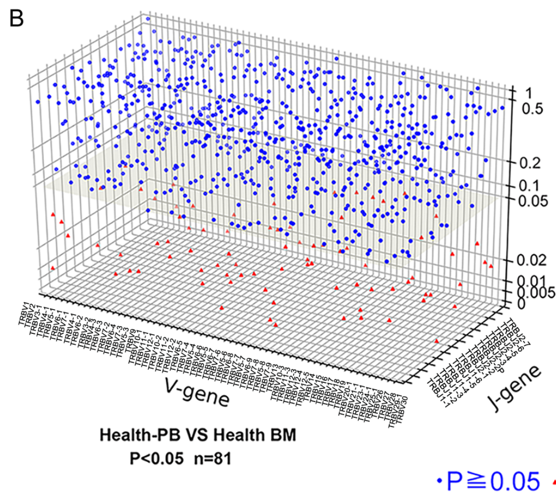

C

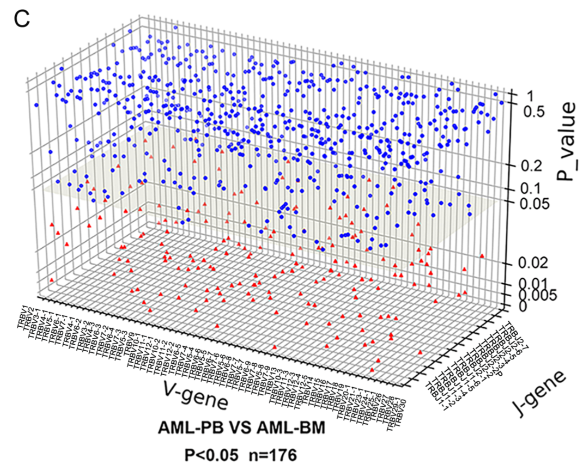

· P≧0.05 · P<0.05

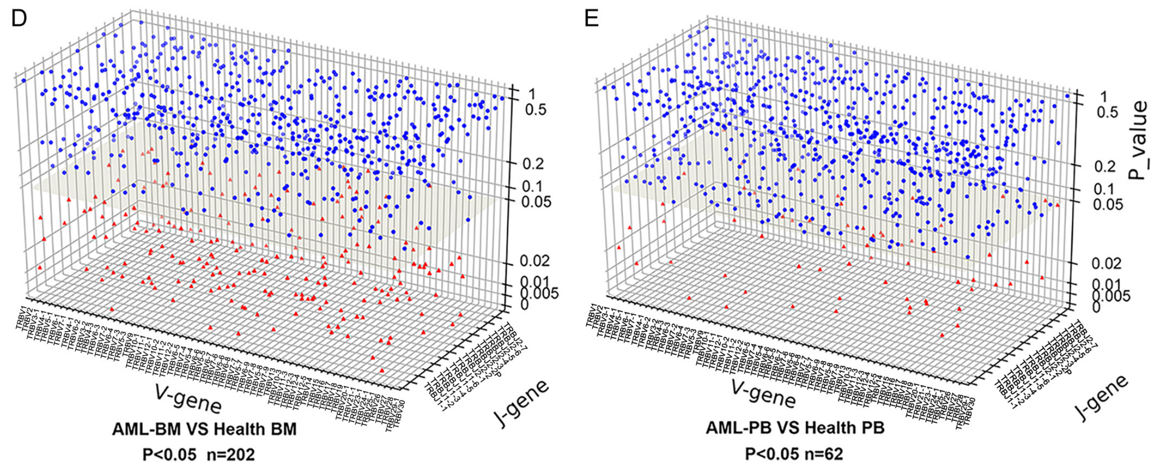

Figure 3. Usage patterns of TCRβ V-J rearrangements in PB and BM CD8+ T cells from AML patients and healthy donors. (A) Dot plots depicting the mean frequency distribution of TCRβ V-J gene rearrangements for CD8+ T cells from the four groups. The variations in TCRβ V-J rearrangements for normal PB vs. healthy BM (B), AML PB vs. AML BM (C), AML BM vs. healthy BM (D), and AML PB vs. healthy PB (E) were investigated. The Mann-Whitney U-test was used to determine whether there were differences between the two groups. Blue circle, $P < 0.05$; red triangle, $P \geq 0.05$.

AML patients but found relatively different usage patterns between BM from healthy donors and BM from AML patients and between PB from AML patients and BM from AML patients (Figure S1). These data suggest that CD8+ T cells in the BM of AML patients exhibit expression of specific TRBV-J rearrangements, indicating that they may recognize bone marrow-specific antigens.

Comparison of identical clonotypes in AML patients and healthy donors

We analyzed the CDR3 amino acid sequences of CD8+ T cells in PB and BM from 31 AML patients and 10 healthy donors to identify the presence of shared clones (i.e., shared CDR3 sequences) in the top 1,000 or 5,000 clones between any two sample pairs (**Figure 4A**). Through intragroup analysis of the CDR3 sequences between different sample pairs, we found a higher ratio of identical T cell clones between sample pairs in the bone marrow of the AML patients (AML BM VS BM, n = 465) when compared to sample pairs in other groups (AML PB VS PB, n = 465 or healthy donor BM VS BM/PB VS PB, n = 45) (**Figure 4B**). Intergroup analysis indicated that there was no difference in the percentage of identical T cell clones between sample pairs from different groups (AML patient BM vs. PB, n = 930; healthy donor BM vs. PB, n = 90; AML patient BM or PB vs. healthy donor BM or PB, n = 310) (**Figure 4C**). By analyzing identical T cell clones in the PB and BM of AML patients or healthy donors (i.e., comparison between BM and PB from the same individual, n = 31 or n = 10), we found that the percentage of identical T cell clones between PB and BM from the same individual was significantly higher than that between peripheral blood and bone marrow among different individuals. Moreover, the percentage of identical T cell clones between PB and paired BM from the healthy donors was significantly higher than that in PB and paired BM from the AML patients (**Figure 4D**). These results suggested that the clonal expansion of BM CD8+ T cells in AML patients was highly specific.

TCRβ repertoire variety and stability among CR patients and relapsed patients

Figure 5A shows BM CD8+ T cell clonal expansion in one relapsed patient and one patient with sustained CR at new diagnosis and after chemotherapy. After discontinuation of chemotherapy, markedly expanded T cell clones were noted in the BM from the relapsed patient but not that from the patient who achieved CR. Looking more deeply into the clonal diversity of the TCRβ repertoires, we found considerably less diversity in the relapse post chemotherapy group than in the other groups (**Figure 5B**). We further calculated the V gene usage of CD8+ T cells in this relapse patient, and the results showed that compared to that at new diagno-

A

HC-BM HC-PB AML-BM AML-PB

TOP 5000 clones

1 → 10 1 → 10 1 → 31 1 → 31

Intergroup Intragroup

TOP 1000 clones

100 50.4 47.9 45.5 43.0 40.5 38.1 35.6 33.1 30.7 28.2 25.7 23.3 20.8 18.3 15.9 1.10 1.00 0.96 0.88 0.80 0.72 0.64 0.56 0.48 0.40 0.32 0.24 0.16 0.08 0

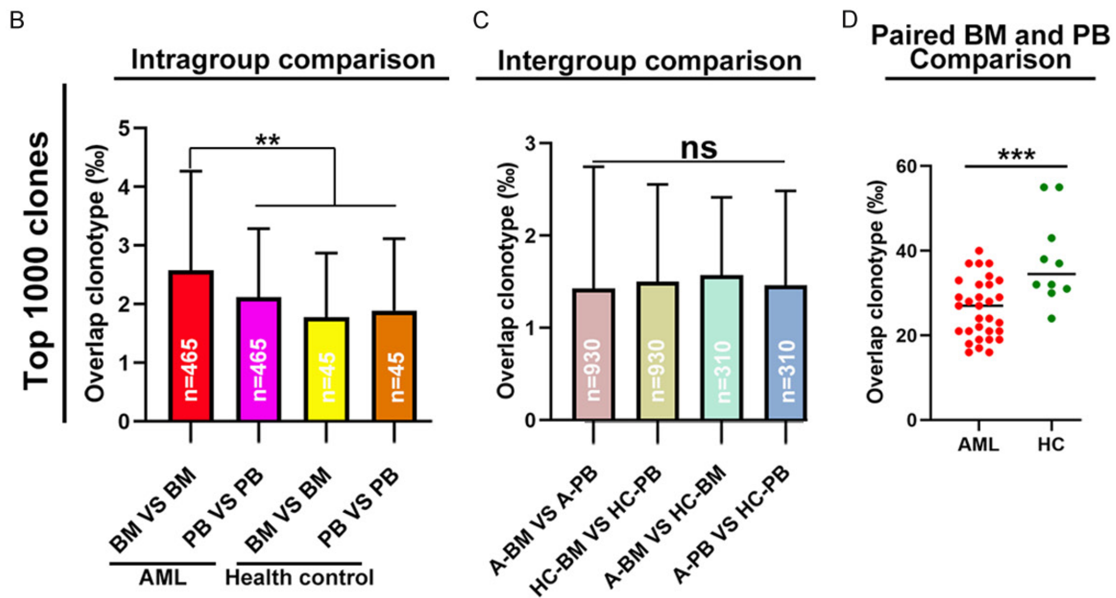

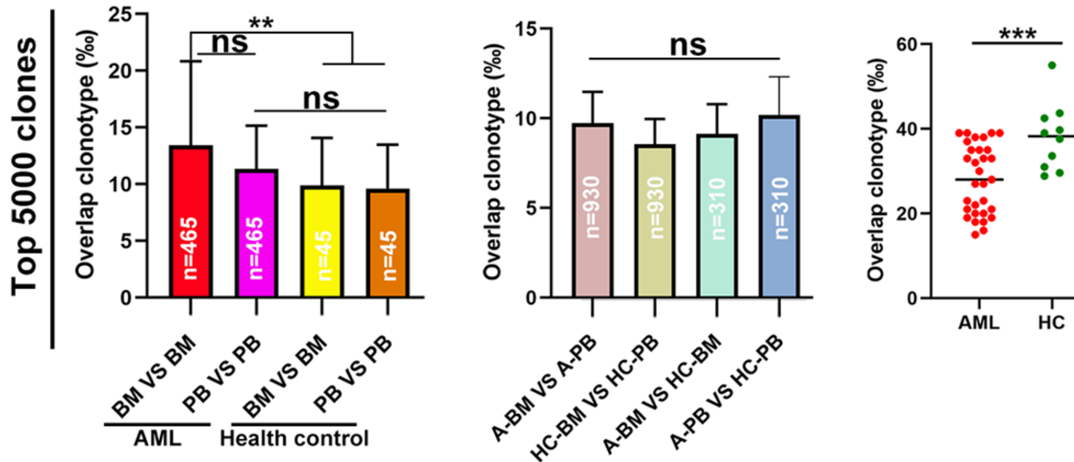

Figure 4. Metrics for TCR β repertoire overlap in PB and BM CD8+ T cells from AML patients and healthy donors. (A) heat map was plotted to assess the similarity of the top 1000 most abundant CDR3 amino acid sequences or the top 5000 most abundant CDR3 amino acid sequences between any two samples. (B) Based on the top 1000 or top 5000 most abundant CDR3 amino acid sequences, repertoire overlap analysis was performed within each group of samples and (C) between groups of samples. (D) Based on the top 1000 or top 5000 most abundant CDR3 amino acid sequences, overlaps between BM and PB from the same individual in AML patients and healthy donors were determined. A dot is used to represent a patient sample. The Mann-Whitney U-test was used to determine whether there were differences between the two groups. Analysis of covariance was initially used for the multiple group comparison. Correction for multiple tests was performed using the false discovery rate method. ns indicates not significant; **$P < 0.05$; ***$P < 0.01$.

sis, the preferential usage pattern of some V gene segments changed dramatically after relapse, and the number of different clones with the same V gene usage was also remarkably different (Figure S2). We further analyzed the Shannon and Gini indexes of BM T cells in all 31 patients at new diagnosis and after chemotherapy. Compared to that at new diagnosis, the Shannon entropy of the relapsed patients showed a marked reduction, whereas the Gini index increased significantly. No difference was observed in the Shannon and Gini indexes in patients with CR (**Figure 5C** and **5D**). By assessing the ratio of identical clones among the top 1,000 T clones in the BM of patients who achieved CR or in patients who experienced relapse at new diagnosis and after treatment, we found that the ratio of identical T clones in the relapsed patients before and after treatment was significantly lower than that in the CR group. However, when we increased the number of clones assessed to 5,000, no difference was observed between the relapse group and the CR group in terms of the ratio of identical T clones at new diagnosis and after chemotherapy (**Figure 5E**). These results showed that compared to those of the AML patients who were in CR after chemotherapy, some of the CD8+ T cells of the patients who relapsed after treatment exhibited massive clonal expansion and reduced clonal diversity, with a significant change in the T cell composition among the top 1,000 clones.

TCR repertoire distribution of CD8+ T cells based on PD-1 expression

Four maturation states of CD8+ T cells were distinguished using CD45RA and CCR7. We found a significantly increased percentage of effector memory T cells (TEM, CD45RA-CCR7-), and CD45RA+ effector memory T cells (TEMRA, CD45RA+CCR7-) and a reduced percentage of naive T cells (T naive, CD45RA+CCR7+) and central memory T cells (TCM, CD45RA-CCR7+), in both peripheral blood and bone marrow of AML patients compared to those of HCs. Meanwhile, the percentage of TEM and TEMRA in bone marrow was higher than in peripheral blood of AML patients (Figure S3A). Following chemotherapy, the percentages of the four subsets had no changes compared to pre-treatment levels (Figure S3B). Several previous reports have suggested the functional involvement of co-inhibitors in AML progression [29-35]. Compared to patients at the time of diagnosis,

A
At new diagnosis
Post chemotherapy
CR patient #14 (Bone marrow)
Relapse patient #8 (Bone marrow)
TRBV2
TRBV3-1
TRBV4-1
TRBV4-2
TRBV4-3
TRBV5-1
TRBV5-4
TRBV5-5
TRBV5-6
TRBV6-1
TRBV10-2
TRBV10-3
TRBV11-1
TRBV11-2
TRBV11-3
TRBV12-3
TRBV12-4
TRBV12-5
TRBV13
TRBV14
TRBV15
TRBV18
TRBV19
TRBV20-1
TRBV23-1
TRBV24-1
TRBV25-1
TRBV28
TRBV29-1
TRBV30

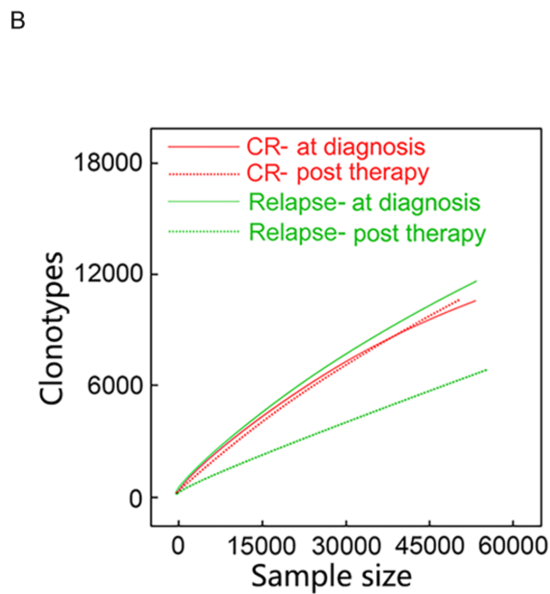
B
CR- at diagnosis
CR- post therapy
Relapse- at diagnosis
Relapse- post therapy
18000
12000
6000
0
Clonotypes
0
15000
30000
45000
60000
Sample size

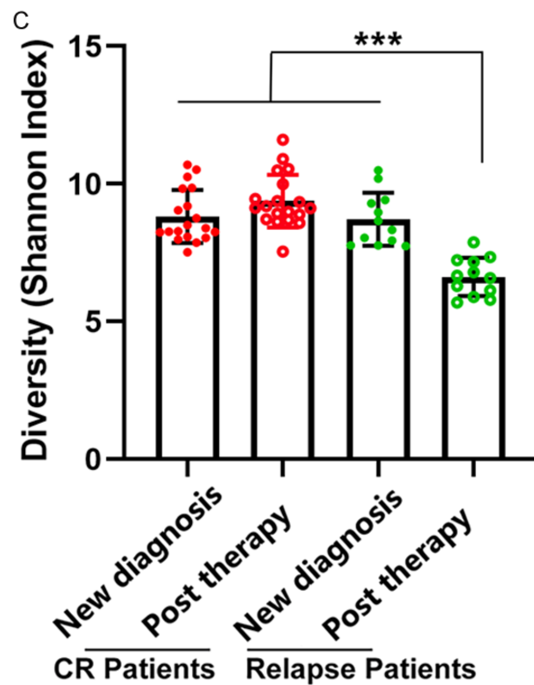
C
Diversity (Shannon Index)
15
10
5
0
***
New diagnosis
Post therapy
New diagnosis
Post therapy
CR Patients
Relapse Patients

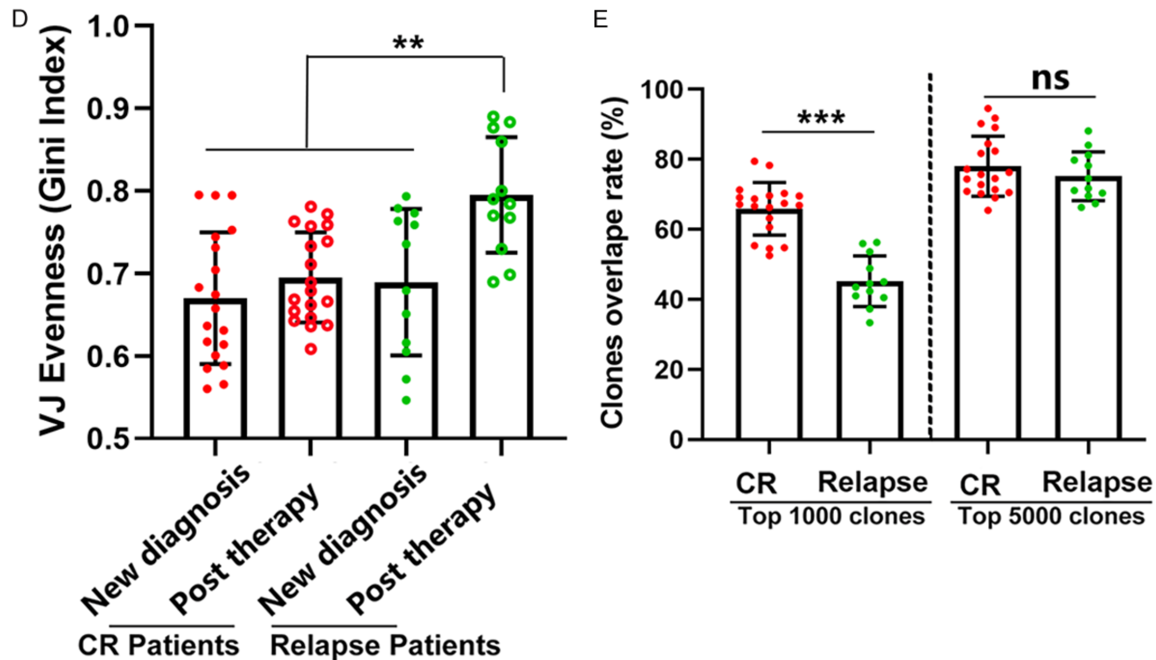

Figure 5. A high degree of clonal expansion in BM $CD8^+$ T cells from relapsed AML patients. (A) Treemap showing the clone repertoires in one patient who relapsed and one patient who remained in remission at new diagnosis and after chemotherapy. Each amino acid sequence was perceived as a separate clonotype, which was represented by a square, and the frequency was indicated by its area; different V genes are represented by different colors. (B) Rarefaction analysis of repertoires from one patient who relapsed and one patient who remained in remission at new diagnosis and after chemotherapy. The number of unique clonotypes in a subsample is plotted against its size (number of TCR cDNA molecules). The diversities of the T cell receptor repertoire in 12 patients who relapsed and 19 patients who had CR after chemotherapy were characterized by computing the Shannon index (C) and the Gini index (D). A dot is used to represent a patient sample. (E) Repertoire overlaps were determined at new diagnosis and after chemotherapy in BM from the same individual based on the top 1000 or top 5000 clonotypes. CR patients: patients who were newly diagnosed with AML and remained in complete remission after chemotherapy. Relapsed patients: patients who were newly diagnosed with AML and relapsed after chemotherapy. The Mann-Whitney U-test was used to determine whether there were differences between the two groups. Analysis of covariance was initially used for the multiple group comparison. Correction for multiple tests was performed using the false discovery rate method. ns indicates not significant; $**P < 0.05$; $***P < 0.01$.

PD-1-, TIGIT- or TIM3-expressing $CD8^+$ T cells displayed a marked increase in BM of relapsed patients and a concomitant decrease in BM of patients who achieved CR (**Figures 6A** and S4).

To determine whether $CD8^+$ $PD\text{-}1^+$ cells exhibited more clonal expansion, TCRβ deep sequencing of $CD8^+$ $PD\text{-}1^+$ and $CD8^+$ $PD\text{-}1^-$ T cells was performed. **Figure 5B-E** depicts the TCR repertoire distribution in 4 samples from one patient who relapsed and one patient who achieved sustained remission at new diagnosis and after chemotherapy. In all the samples analyzed, $CD8^+$ $PD\text{-}1^+$ T cells were found to be more oligoclonal than $CD8^+$ $PD\text{-}1^-$ T cells. The cumulative frequency of the top 50 clonotypes was 42.9%, 35.9%, 41.5%, and 50% of the total $PD\text{-}1^+$ T cells at the time of CR diagnosis, CR post chemotherapy, relapse diagnosis, and relapse post chemotherapy, respectively, but only 18.2%, 15.8%, 20.4%, and 29.6% of the total $PD\text{-}1^-$ frequency at the time of CR diagnosis, CR post chemotherapy, relapse diagnosis, and relapse post chemotherapy, respectively (**Figure 6B** and **6D**). We further analyzed the distribution of the top 50 clonotypes among $CD8^+$ $PD\text{-}1^+$ cells and $CD8^+$ $PD\text{-}1^-$ T cells in bulk $CD8^+$ T cells based on previous results for these two patients. Both at diagnosis and after chemotherapy, the clones with a higher frequency and the overall frequency of the top 50 clonotypes in the $CD8^+$ $PD\text{-}1^+$ group were higher than those in the $CD8^+$ $PD\text{-}1^-$ group (**Figure 6C** and **6E**; Tables S2, S3, S4 and S5). Moreover, the top 50 prevalent clonotypes in the $CD8^+$ $PD\text{-}1^+$ group were far less frequent in the $PD\text{-}1^-$ group

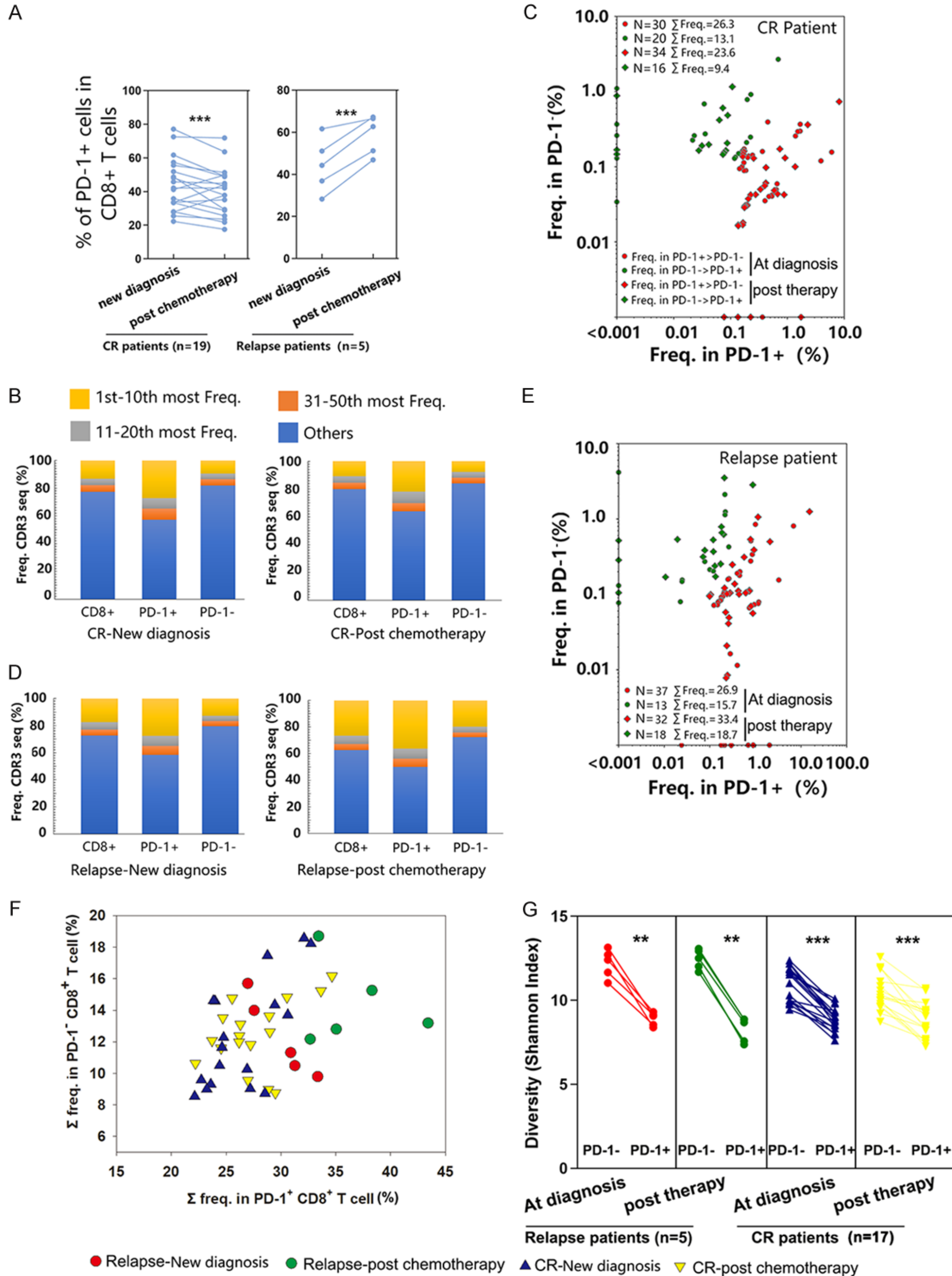

Figure 6. TCR repertoire distribution of CD8+ T cells based on PD-1 expression in CR and relapsed AML patients. (A) Expression of PD-1 was determined by flow cytometry. Samples from 5 patients who relapsed and 19 patients who had CR after chemotherapy were collected for flow cytometry analysis. (B-F) The clonotype distribution of CD8+ T cells was associated with PD-1 expression. CD8+ T cells were sorted from one patient who had CR (B and C) and one relapsed patient (D and E) based on the expression of PD-1. mRNA extraction and deep sequencing of TCRβ CDR3 were performed. (B and D) Analysis of TCRβ repertoire clonal frequency in CD8+ (as shown above), CD8+ PD-1+ (4 ×

10^4 cells), and $CD8^+$ PD-1^- (4×10^4 cells) T cells. The abundances of the top 1 to 10, 11 to 20, and 21 to 50 clonotypes, as well as the remaining clonotypes, are shown. (C and E) The distribution of the top 50 most frequent clonotypes among $CD8^+$ T cells was compared between the $CD8^+$ PD-1^+ populations and $CD8^+$ PD-1^- populations. Each dot represents a clonotype from a newly diagnosed sample; each rhombus represents a clonotype from a sample post chemotherapy. Red represents the frequency of clonotypes in $CD8^+$ PD-1^+ > $CD8^+$ PD-1^-; green represents the frequency of clonotypes in $CD8^+$ PD-1^- > $CD8^+$ PD-1^+. The total frequency (Σ freq.) of the clonotypes in each population is cumulative. (F) The top 50 clonotypes in $CD8^+$ T cells were frequently distributed in the $CD8^+$ PD-1^+ and $CD8^+$ PD-1^- populations. Red dots represent samples collected at new diagnosis from patients who relapsed post chemotherapy; green dots represent samples collected after treatment from patients who relapsed post chemotherapy; blue triangles represent samples collected at new diagnosis from patients with sustained CR post chemotherapy; yellow triangles represent samples collected after treatment from patients with sustained CR post chemotherapy; $CD8^+$ PD-1^- and $CD8^+$ PD-1^+ T cell from 5 patients who relapsed and 17 patients who had CR after chemotherapy were collected for TCRβ CDR3 sequencing. (G) Shannon index comparison between $CD8^+$ PD-1^+ and $CD8^+$ PD-1^- populations. The Wilcoxon signed-rank test was used for matched paired comparisons. $^{**}P < 0.05$; $^{***}P < 0.01$.

(Figure S5). Analysis of all samples from the 5 relapsed patients and 17 CR patients also revealed that the top 50 clonotypes in each $CD8^+$ population were more frequent in the $CD8^+$ PD-1^+ group than in the $CD8^+$ PD-1^- group (**Figure 6F**). There were significant reductions in the Shannon index in the $CD8^+$ PD-1^+ group compared to the $CD8^+$ PD-1^- group, indicating lower TCR repertoire diversity in the $CD8^+$ PD-1^+ group (**Figure 6G**).

Discussion

$CD8^+$ T cells are cytotoxic effector cells of the immune system that are involved in cell-mediated immunity. Cytotoxic T lymphocyte (CTL) reactivity depends mainly on the hypervariable TCR heterodimer CDR3, which is composed of TCRα and TCRβ chains and is responsible for recognition of cell surface MHC-peptide complexes [36]. Currently, our understanding of TCR repertoires in $CD8^+$ T cells and the effect of chemotherapy on TCR repertoires in AML is still lacking. We performed a comprehensive analysis of TCR repertoires in PB and BM $CD8^+$ T cells from 10 healthy donors and 31 AML patients at diagnosis and after chemotherapy. The results reveal (i) diminished TCR repertoire diversity and increased clonal expansion in AML BM but not PB; (ii) a higher identical clone ratio in AML BM; (iii) higher T cell clonal expansion post chemotherapy in relapsed patients compared to patients at new diagnosis; and (iv) greater expansion and lower diversity of TCRβ clonotypes in $CD8^+$ PD-1^+ T cells than in $CD8^+$ PD-1^- T cells.

In the present study, we observed greater clonal expansion of $CD8^+$ T cells in BM but not in PB of AML patients compared to healthy donors. Zhang et al. reported higher clonal expansion of both T cells and B cells in the PB of AML patients [15]. In contrast to their findings, we did not find clonal expansion of $CD8^+$ T cells in the PB of AML patients. This may be due to the different methods used for obtaining TCR sequences and the heterogeneity of the samples. We obtained approximately 3,280,000 unique $CD8^+$ TCRβ CDR3 sequences from 82 samples by using the target amplification method; in comparison, Zhang et al. obtained 225,000 CDR3 sequences for the TCR α, β, γ, and δ chains and 1,210,000 CDR3 sequences for the B cell immunoglobulin (Ig) heavy and light chains from unselected bulk tumor RNA-seq data from 369 samples. Based on the data characteristics, we were able to better assess $CD8^+$ T cell clones, whereas Zhang et al. could analyze the overall T cell ($CD4^+$ T cells and $CD8^+$ T cells) clone characteristics based on a larger sample size. At the same time, we found that compared with healthy donors, AML patients had a lower rate of identical $CD8^+$ T cell clones between the BM and their own PB. In addition, compared to those at the time of diagnosis, the Top 1000 $CD8^+$ T cell clones in the BM of patients who relapsed after chemotherapy showed greater changes. Originating from myeloid hematopoietic progenitors, AML cells can grow and differentiate within the BM microenvironment [37]. Additionally, the BM has been proven to be a preferential site for T cells specific for blood-borne or non-small-cell lung cancer-associated antigens [38, 39]. These features may support our notion that $CD8^+$ T cell clones in the BM of AML patients have special characteristics.

Several studies reported increased levels of PD-1 as well as multiple co-expressed inhibitor receptors (IRs) on $CD8^+$ T cells of AML patients at diagnosis [19, 40]. Longitudinal observation

of changes in the co-inhibitor receptors expression pattern from our study and others indicated that PD-1 and TIM3, together with several other co-inhibitory receptors, are increased in BM CD8+ T cells in non-responders and reduced in responders post chemotherapy [2, 33]. Our analysis of TCRβ sequences showed that TCRβ clonotypes in CD8+ PD-1+ populations were more oligoclonal than those in CD8+ PD-1- T populations. These observations highlight the importance of further evaluating TCR clonotypic frequency and unique phenotypic traits of CD8+ T cells in AML to identify patient-specific repertoires of tumor-reactive CD8+ lymphocytes. For therapies that require isolation of T cells expressing inhibitory receptors [41, 42], T cell exhaustion and dysfunction pose a major challenge. However, the present study and other recently published works suggested that CD8+ PD-1+ cells underwent extensive clonal expansion [21], produced IFN-γ and lysed tumors in vitro [19]. This adds to evidence that the process of T cell dysfunction associated with co-expressed inhibitory receptors is reversible and that the enrichment of tumor-reactive cells for patient treatment is reproducible.

Our study has several limitations. First, high disease heterogeneity and a small sample size may have limited our ability to uncover specific CDR3 amino sequences as biomarkers for AML characteristics or determine the exact correlation between the baseline TCR repertoire diversity and prognosis. Second, isolation of the patient-specific repertoire of tumor-reactive CD8+ T cells was not performed, so the anti-leukemia effect was not evaluated. AML is characterized by reduced immunogenicity and has one of the lowest mutation rates compared to other cancer types [43]; nevertheless, it is the quality of mutations, not the mutational burden, that may be of more significance in enhancing immune functions. Several other studies have shown that *NPM1* mutation-related TCRs correlate with enhanced anticancer effects and improved clinical outcomes [44, 45]. Thus, isolation and recognition of antigens derived from common AML mutations such as those in *NPM1*, *DNMT3A*, and *FLT3*, identification of TCRs that can recognize these antigens, and analysis of related TCRs in patients may be the logical starting point for the implementation of immunotherapy in AML. Third, owing to the limited sample availability, a comprehensive comparison between patients at new diagnosis and patients after chemotherapy was difficult. Extensive analysis of the TCR repertoire differences in relapsed patients before and after chemotherapy would provide valuable information, and further studies should be carried out on this topic.

Conclusions

Our findings provide the first objective data characterizing the signatures of the CD8+ TCR repertoire at diagnosis and after chemotherapy in patients with AML. Sequence analysis of CDR3 has shown that CD8+ T cells in the BM of AML patients display specific TCRβ clonal expansion, and more expansion is found in patients who relapse after chemotherapy and among PD-1+ T cells. The antitumor reactivity of individual TCRs can be harnessed in the future to develop tailored T cell therapies for AML patients, and understanding immune responses to chemotherapy is thus crucial for the development and use of immunotherapies to treat patients with AML.

Acknowledgements

This study was supported by the National Natural Science Foundation of China (Grant Nos. 81660616 and 81960032), The Social Development Research Project of Guiczhou Province (Grant No. [2015]3036) and National Center for clinical medicine of hematological diseases (2020ZKPB03). We thank Drs. Wenqiang Zhang and Feng Ye for offering their insights and advice on this project.

Disclosure of conflict of interest

None.

Address correspondence to: Jishi Wang, Department of Hematology, Affiliated Hospital of Guizhou Medical University, No. 9 Beijing Street, Yunyan District, Guiyang 550004, Guizhou Province, China. Tel: +86-0851-86770494; Fax: +86-0851-86757898; E-mail: wangjishi9646@163.com

References

[1] Ferrara F and Schiffer CA. Acute myeloid leukaemia in adults. Lancet 2013; 381: 484-495.

[2] Knaus HA, Berglund S, Hackl H, Blackford AL, Zeidner JF, Montiel-Esparza R, Mukhopadhyay R, Vanura K, Blazar BR, Karp JE, Luznik L and

Gojo I. Signatures of CD8+ T cell dysfunction in AML patients and their reversibility with response to chemotherapy. JCI Insight 2018; 3: e120974.

[3] Khalil DN, Smith EL, Brentjens RJ and Wolchok JD. The future of cancer treatment: immunomodulation, CARs and combination immunotherapy. Nat Rev Clin Oncol 2016; 13: 394.

[4] Kenderian SS, Ruella M, Shestova O, Klichinsky M, Aikawa V, Morrissette JJ, Scholler J, Song D, Porter DL, Carroll M, June CH and Gill S. CD33-specific chimeric antigen receptor T cells exhibit potent preclinical activity against human acute myeloid leukemia. Leukemia 2015; 29: 1637-1647.

[5] Casucci M, Nicolis di Robilant B, Falcone L, Camisa B, Norelli M, Genovese P, Gentner B, Gullotta F, Ponzoni M, Bernardi M, Marcatti M, Saudemont A, Bordignon C, Savoldo B, Ciceri F, Naldini L, Dotti G, Bonini C and Bondanza A. CD44v6-targeted T cells mediate potent antitumor effects against acute myeloid leukemia and multiple myeloma. Blood 2013; 122: 3461-3472.

[6] Daver N, Garcia-Manero G, Basu S, Boddu PC, Alfayez M, Cortes JE, Konopleva M, Ravandi-Kashani F, Jabbour E, Kadia T, Nogueras-Gonzalez GM, Ning J, Pemmaraju N, DiNardo CD, Andreeff M, Pierce SA, Gordon T, Kornblau SM, Flores W, Alhamal Z, Bueso-Ramos C, Jorgensen JL, Patel KP, Blando J, Allison JP, Sharma P and Kantarjian H. Efficacy, safety, and biomarkers of response to azacitidine and nivolumab in relapsed/refractory acute myeloid leukemia: a nonrandomized, open-label, phase ii study. Cancer Discov 2019; 9: 370-383.

[7] Gill S, Tasian SK, Ruella M, Shestova O, Li Y, Porter DL, Carroll M, Danet-Desnoyers G, Scholler J, Grupp SA, June CH and Kalos M. Preclinical targeting of human acute myeloid leukemia and myeloablation using chimeric antigen receptor-modified T cells. Blood 2014; 123, 2343-2354

[8] Tawara I, Kageyama S, Miyahara Y, Fujiwara H, Nishida T, Akatsuka Y, Ikeda H, Tanimoto K, Terakura S, Murata M, Inaguma Y, Masuya M, Inoue N, Kidokoro T, Okamoto S, Tomura D, Chono H, Nukaya I, Mineno J, Naoe T, Emi N, Yasukawa M, Katayama N and Shiku H. Safety and persistence of WT1-specific T-cell receptor gene-transduced lymphocytes in patients with AML and MDS. Blood 2017; 130: 1985-1994.

[9] Perna F, Berman SH, Soni RK, Mansilla-Soto J, Eyquem J, Hamieh M, Hendrickson RC, Brennan CW and Sadelain M. Integrating proteomics and transcriptomics for systematic combinatorial chimeric antigen receptor therapy of AML. Cancer Cell 2017; 32: 506-519, e505.

[10] Kim MY, Yu KR, Kenderian SS, Ruella M, Chen S, Shin TH, Aljanahi AA, Schreeder D, Klichinsky M, Shestova O, Kozlowski MS, Cummins KD, Shan X, Shestov M, Bagg A, Morrissette JJD, Sekhri P, Lazzarotto CR, Calvo KR, Kuhns DB, Donahue RE, Behbehani GK, Tsai SQ, Dunbar CE and Gill S. Genetic inactivation of CD33 in hematopoietic stem cells to enable CAR T cell immunotherapy for acute myeloid leukemia. Cell 2018; 173: 1439-1453, e1419.

[11] Reiser J and Banerjee A. Effector, memory, and dysfunctional CD8(+) T cell fates in the antitumor immune response. J Immunol Res 2016; 2016: 8941260.

[12] Cole DK, Miles KM, Madura F, Holland CJ, Schauenburg AJ, Godkin AJ, Bulek AM, Fuller A, Akpovwa HJ, Pymm PG, Liddy N, Sami M, Li Y, Rizkallah PJ, Jakobsen BK and Sewell AK. T-cell receptor (TCR)-peptide specificity overrides affinity-enhancing TCR-major histocompatibility complex interactions. J Biol Chem 2014; 289: 628-638.

[13] Fozza C, Barraqueddu F, Corda G, Contini S, Virdis P, Dore F, Bonfigli S and Longinotti M. Study of the T-cell receptor repertoire by CDR3 spectratyping. J Immunol Methods 2017; 440: 1-11.

[14] Jin Z, Luo Q, Lu S, Wang X, He Z, Lai J, Chen S, Yang L, Wu X and Li Y. Oligoclonal expansion of TCR Vdelta T cells may be a potential immune biomarker for clinical outcome of acute myeloid leukemia. J Hematol Oncol 2016; 9: 126.

[15] Zhang J, Hu X, Wang J, Sahu AD, Cohen D, Song L, Ouyang Z, Fan J, Wang B, Fu J, Gu S, Sade-Feldman M, Hacohen N, Li W, Ying X, Li B and Liu XS. Immune receptor repertoires in pediatric and adult acute myeloid leukemia. Genome Med 2019; 11: 73.

[16] Morath A and Schamel WW. alphabeta and gammadelta T cell receptors: similar but different. J Leukoc Biol 2020; 107: 1045-1055.

[17] Han J, Duan J, Bai H, Wang Y, Wan R, Wang X, Chen S, Tian Y, Wang D, Fei K, Yao Z, Wang S, Lu Z, Wang Z and Wang J. TCR repertoire diversity of peripheral $PD\text{-}1^+$ $CD8^+$ T cells predicts clinical outcomes after immunotherapy in patients with non-small cell lung cancer. Cancer Immunol Res 2020; 8: 146-154.

[18] Sharpe AH and Pauken KE. The diverse functions of the PD1 inhibitory pathway. Nat Rev Immunol 2018; 18: 153-167.

[19] Jia B, Wang L, Claxton DF, Ehmann WC, Rybka WB, Mineishi S, Rizvi S, Shike H, Bayerl M, Schell TD, Hohl RJ and Zheng H. Bone marrow CD8 T cells express high frequency of PD-1 and exhibit reduced anti-leukemia response in newly diagnosed AML patients. Blood Cancer J 2018; 8: 34.

[20] Laszlo GS, Gudgeon CJ, Harrington KH and Walter RB. T-cell ligands modulate the cytolytic

activity of the CD33/CD3 BiTE antibody construct, AMG 330. Blood Cancer J 2015; 5: e340.
[21] Gros A, Robbins PF, Yao X, Li YF, Turcotte S, Tran E, Wunderlich JR, Mixon A, Farid S, Dudley ME, Hanada K, Almeida JR, Darko S, Douek DC, Yang JC and Rosenberg SA. PD-1 identifies the patient-specific CD8(+) tumor-reactive repertoire infiltrating human tumors. J Clin Invest 2014; 124: 2246-2259.
[22] Han J, Duan J, Bai H, Wang Y, Wan R, Wang X, Chen S, Tian Y, Wang D, Fei K, Yao Z, Wang S, Lu Z, Wang Z and Wang J. TCR repertoire diversity of peripheral PD-1(+)CD8(+) T cells predicts clinical outcomes after immunotherapy in patients with non-small cell lung cancer. Cancer Immunol Res 2020; 8: 146-154.
[23] Glanville J, Huang H, Nau A, Hatton O, Wagar LE, Rubelt F, Ji X, Han A, Krams SM, Pettus C, Haas N, Arlehamn CSL, Sette A, Boyd SD, Scriba TJ, Martinez OM and Davis MM. Identifying specificity groups in the T cell receptor repertoire. Nature 2017; 547: 94-98.
[24] Zhang L, Cham J, Paciorek A, Trager J, Sheikh N and Fong L. 3D: diversity, dynamics, differential testing - a proposed pipeline for analysis of next-generation sequencing T cell repertoire data. BMC Bioinformatics 2017; 18: 129.
[25] Shugay M, Bagaev DV, Zvyagin IV, Vroomans RM, Crawford JC, Dolton G, Komech EA, Sycheva AL, Koneva AE, Egorov ES, Eliseev AV, Van Dyk E, Dash P, Attaf M, Rius C, Ladell K, McLaren JE, Matthews KK, Clemens EB, Douek DC, Luciani F, van Baarle D, Kedzierska K, Kesmir C, Thomas PG, Price DA, Sewell AK and Chudakov DM. VDJdb: a curated database of T-cell receptor sequences with known antigen specificity. Nucleic Acids Res 2018; 46: D419-D427.
[26] Nazarov VI, Pogorelyy MV, Komech EA, Zvyagin IV, Bolotin DA, Shugay M, Chudakov DM, Lebedev YB and Mamedov IZ. tcR: an R package for T cell receptor repertoire advanced data analysis. BMC Bioinformatics 2015; 16: 175.
[27] Di Lorenzo B, Ravens S and Silva-Santos B. High-throughput analysis of the human thymic Vdelta1(+) T cell receptor repertoire. Sci Data 2019; 6: 115.
[28] Schloss PD, Westcott SL, Ryabin T, Hall JR, Hartmann M, Hollister EB, Lesniewski RA, Oakley BB, Parks DH, Robinson CJ, Sahl JW, Stres B, Thallinger GG, Van Horn DJ and Weber CF. Introducing mothur: open-source, platform-independent, community-supported software for describing and comparing microbial communities. Appl Environ Microbiol 2009; 75: 7537-7541.
[29] Han Y, Liu X, Wang Y, Wu X, Guan Y, Li H, Chen X, Zhou B, Yuan Q, Ou Y, Wu R, Huang W, Wang Y, Zhang M, Zhang Y, Zhu D, Zhu H, Yang L, Yi X, Huang C and Huang J. Identification of characteristic TRB V usage in HBV-associated HCC by using differential expression profiling analysis. Oncoimmunology 2015; 4: e1021537.
[30] Casucci M, Di Robilant BN, Falcone L, Camisa B, Norelli M, Genovese P, Gentner B, Gullotta F, Ponzoni M, Bernardi M, Marcatti M, Saudemont A, Bordignon C, Savoldo B, Ciceri F, Naldini L, Dotti G, Bonini C and Bondanza A. CD44v6-targeted T cells mediate potent antitumor effects against acute myeloid leukemia and multiple myeloma. Blood 2013; 122: 3461-3472.
[31] Reiser J and Banerjee A. Effector, memory, and dysfunctional CD8+ T cell fates in the antitumor immune response. J Immunol Res 2016; 2016: 8941260.
[32] Gill S, Tasian SK, Ruella M, Shestova O, Li Y, Porter DL, Carroll M, Danet-Desnoyers G, Scholler J, Grupp SA, June CH and Kalos M. Preclinical targeting of human acute myeloid leukemia and myeloablation using chimeric antigen receptor-modified T cells. Blood 2014; 123: 2343-2354.
[33] Dama P, Tang M, Fulton N, Kline J and Liu H. Gal9/Tim-3 expression level is higher in AML patients who fail chemotherapy. J Immunother Cancer 2019; 7: 175.
[34] Kong Y, Zhang J, Claxton DF, Ehmann WC, Rybka WB, Zhu L, Zeng H, Schell TD and Zheng H. PD-1(hi)TIM-3(+) T cells associate with and predict leukemia relapse in AML patients post allogeneic stem cell transplantation. Blood Cancer J 2015; 5: e330.
[35] Kong Y, Zhu L, Schell TD, Zhang J, Claxton DF, Ehmann WC, Rybka WB, George MR, Zeng H and Zheng H. T-cell immunoglobulin and ITIM domain (TIGIT) associates with CD8+ T-cell exhaustion and Poor Clinical Outcome in AML patients. Clin Cancer Res 2016; 22: 3057-3066.
[36] Chen G, Yang X, Ko A, Sun X, Gao M, Zhang Y, Shi A, Mariuzza RA and Weng NP. Sequence and structural analyses reveal distinct and highly diverse human CD8(+) TCR repertoires to immunodominant viral antigens. Cell Rep 2017; 19: 569-583.
[37] Shafat MS, Gnaneswaran B, Bowles KM and Rushworth SA. The bone marrow microenvironment - home of the leukemic blasts. Blood Rev 2017; 31: 277-286.
[38] Feuerer M, Beckhove P, Garbi N, Mahnke Y, Limmer A, Hommel M, Hammerling GJ, Kyewski B, Hamann A, Umansky V and Schirrmacher V. Bone marrow as a priming site for T-cell responses to blood-borne antigen. Nat Med 2003; 9: 1151-1157.
[39] Safi S, Yamauchi Y, Stamova S, Rathinasamy A, Op den Winkel J, Junger S, Bucur M, Umansky L, Warth A, Herpel E, Eichhorn M, Winter H,

Hoffmann H and Beckhove P. Bone marrow expands the repertoire of functional T cells targeting tumor-associated antigens in patients with resectable non-small-cell lung cancer. Oncoimmunology 2019; 8: e1671762.

[40] Williams P, Basu S, Garcia-Manero G, Hourigan CS, Oetjen KA, Cortes JE, Ravandi F, Jabbour EJ, Al-Hamal Z, Konopleva M, Ning J, Xiao L, Hidalgo Lopez J, Kornblau SM, Andreeff M, Flores W, Bueso-Ramos C, Blando J, Galera P, Calvo KR, Al-Atrash G, Allison JP, Kantarjian HM, Sharma P and Daver NG. The distribution of T-cell subsets and the expression of immune checkpoint receptors and ligands in patients with newly diagnosed and relapsed acute myeloid leukemia. Cancer 2018; 125: 1470-1481.

[41] Farhood B, Najafi M and Mortezaee K. CD8(+) cytotoxic T lymphocytes in cancer immunotherapy: a review. J Cell Physiol 2019; 234: 8509-8521.

[42] Durgeau A, Virk Y, Corgnac S and Mami-Chouaib F. Recent advances in targeting CD8 T-Cell immunity for more effective cancer immunotherapy. Front Immunol 2018; 9: 14.

[43] Cancer Genome Atlas Research Network, Ley TJ, Miller C, Ding L, Raphael BJ, Mungall AJ, Robertson A, Hoadley K, Triche TJ Jr, Laird PW, Baty JD, Fulton LL, Fulton R, Heath SE, Kalicki-Veizer J, Kandoth C, Klco JM, Koboldt DC, Kanchi KL, Kulkarni S, Lamprecht TL, Larson DE, Lin L, Lu C, McLellan MD, McMichael JF, Payton J, Schmidt H, Spencer DH, Tomasson MH, Wallis JW, Wartman LD, Watson MA, Welch J, Wendl MC, Ally A, Balasundaram M, Birol I, Butterfield Y, Chiu R, Chu A, Chuah E, Chun HJ, Corbett R, Dhalla N, Guin R, He A, Hirst C, Hirst M, Holt RA, Jones S, Karsan A, Lee D, Li HI, Marra MA, Mayo M, Moore RA, Mungall K, Parker J, Pleasance E, Plettner P, Schein J, Stoll D, Swanson L, Tam A, Thiessen N, Varhol R, Wye N, Zhao Y, Gabriel S, Getz G, Sougnez C, Zou L, Leiserson MD, Vandin F, Wu HT, Applebaum F, Baylin SB, Akbani R, Broom BM, Chen K, Motter TC, Nguyen K, Weinstein JN, Zhang N, Ferguson ML, Adams C, Black A, Bowen J, Gastier-Foster J, Grossman T, Lichtenberg T, Wise L, Davidsen T, Demchok JA, Shaw KR, Sheth M, Sofia HJ, Yang L, Downing JR and Eley G. Genomic and epigenomic landscapes of adult de novo acute myeloid leukemia. N Engl J Med 2013; 368: 2059-2074.

[44] van der Lee DI, Reijmers RM, Honders MW, Hagedoorn RS, de Jong RC, Kester MG, van der Steen DM, de Ru AH, Kweekel C, Bijen HM, Jedema I, Veelken H, van Veelen PA, Heemskerk MH, Falkenburg JHF and Griffioen M. Mutated nucleophosmin 1 as immunotherapy target in acute myeloid leukemia. J Clin Invest 2019; 129: 774-785.

[45] Greiner J, Ono Y, Hofmann S, Schmitt A, Mehring E, Gotz M, Guillaume P, Dohner K, Mytilineos J, Dohner H and Schmitt M. Mutated regions of nucleophosmin 1 elicit both CD4(+) and CD8(+) T-cell responses in patients with acute myeloid leukemia. Blood 2012; 120: 1282-1289.

Table S1. AML Patients and Donors characteristics

Domain	Patients Total (n = 31)	Donors Total (n = 10)
Age (y)		
Median	47	40
Range	23-74	34-46
Gender		
Male	17	5
Female	14	5
WBC (× 10^9/L)		
Mean	27.91	6.17
Range	6.38-63.72	5.24-7.72
PB blasts (%)		
Mean	33.29	
Range	21-56	
PB Absolute blasts count (× 10^9/L)		
Mean	9.94	
Range	1.54-29.94	
BM blasts (%)		
Mean	66.23	
Range	27-95	
BM Absolute blasts count (× 10^9/L)		
Mean	18.76	
Range	3.08-47.71	
Moleculars		
FLT3-ITD	16.13%	
NPM1	19.35%	
TP53	6.45%	
Cytogenetics		
Favorable	22.58%	
Intermediate	58.07%	
Adverse	19.35%	

WBC, white blood cell; PB, peripheral blood; BM, bone marrow. AML type accords to WHO (World Health Organization) 2016.

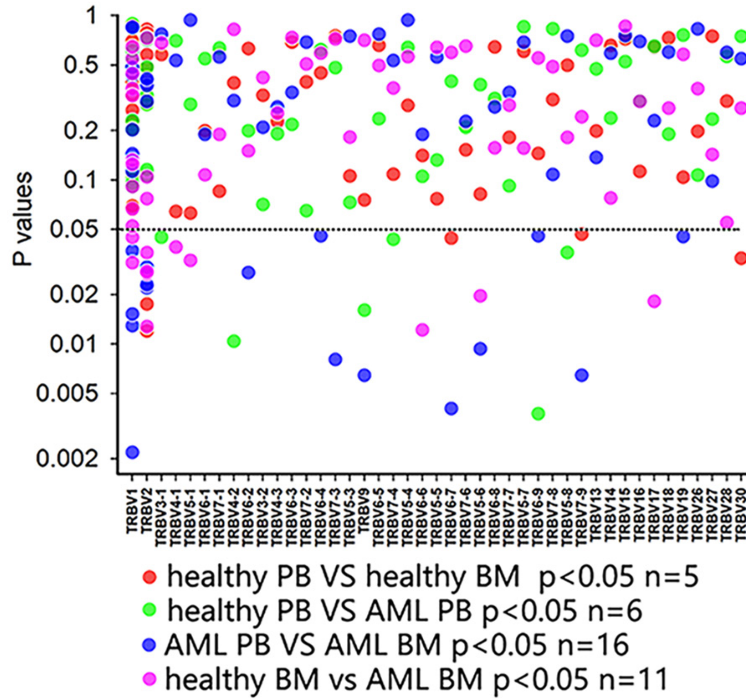

Figure S1. Comparison of overall usage of TCRβ V gene segments in AML patients and healthy donors. Differences in the frequencies of TRβ V gene segments in normal PB vs. normal BM, AML PB vs. AML BM, AML BM vs. normal BM, and AML PB vs. normal PB. Four study groups containing BM (n = 31) and PB (n = 31) samples obtained from AML patients and BM (n = 10) and PB (n = 10) samples obtained from healthy donors.

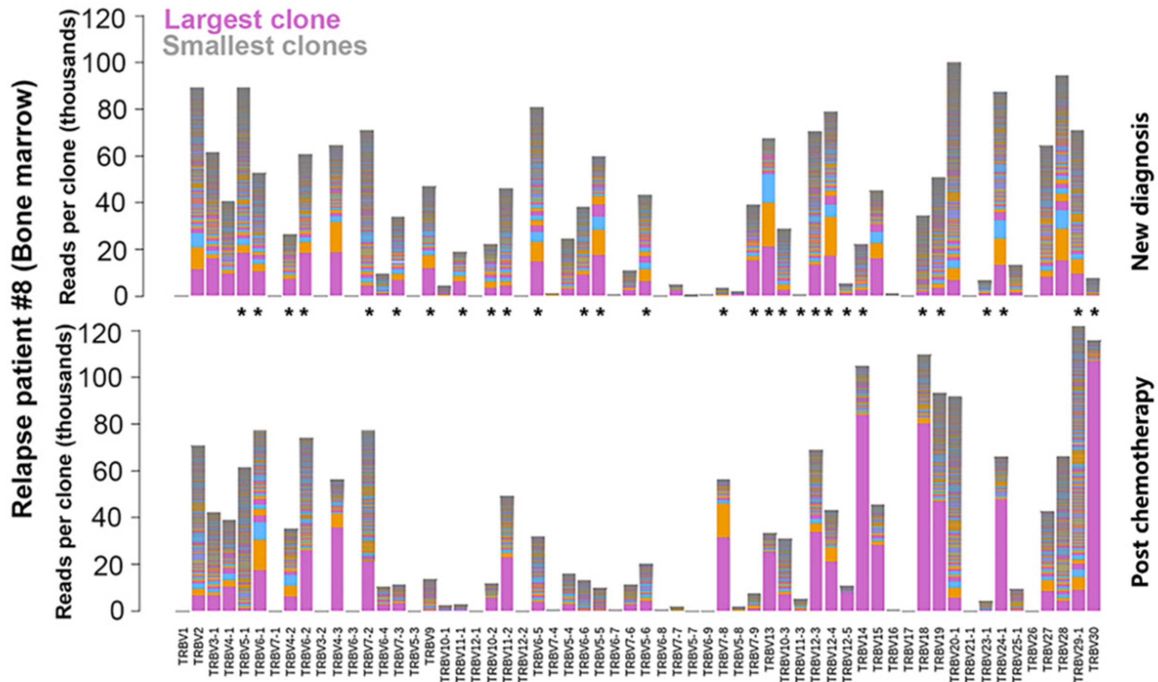

Figure S2. The usage pattern of V gene segments in the relapsed patient (#8) at new diagnosis and post chemotherapy. Color segments within each bar indicate the contribution of individual clones, arranged from the smallest clones (gray, top) to the largest clones (purple, bottom). The Mann-Whitney U-test was used to for comparisons between two groups. * indicates $P < 0.01$.

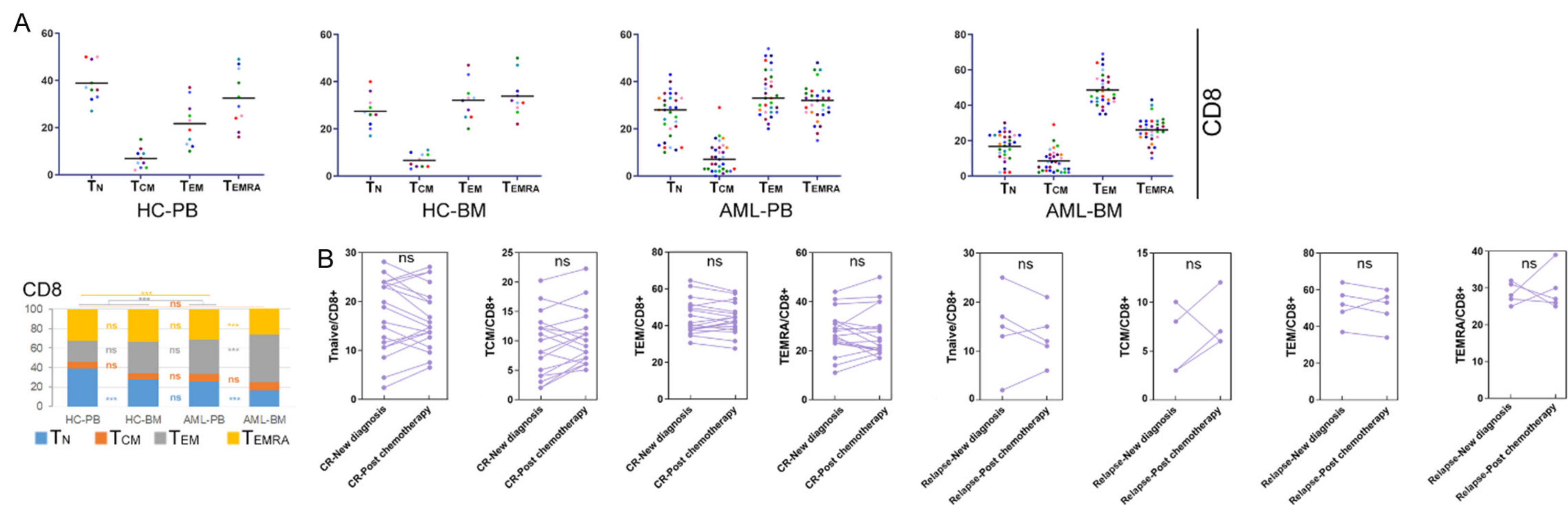

Figure S3. Phenotypical analysis of CD8⁺ T cells from healthy donors and AML patients. CD8⁺ T cell subsets were analyzed by multiparameter flow cytometry according to the expression of CD45RA and CCR7. A. Phenotypical features of BM and PB T cells from newly diagnosed AML patients (n = 31) and healthy controls (HCs) (n = 10). B. Phenotypical features of BM T cells from patients before and after chemotherapy. Samples collected from patients who relapsed (n = 5) and patients who achieved CR (n = 19) after chemotherapy. The Mann-Whitney U-test was used to for comparisons between two groups. The Wilcoxon signed-rank test was used for matched paired comparisons. *** indicates P < 0.01.

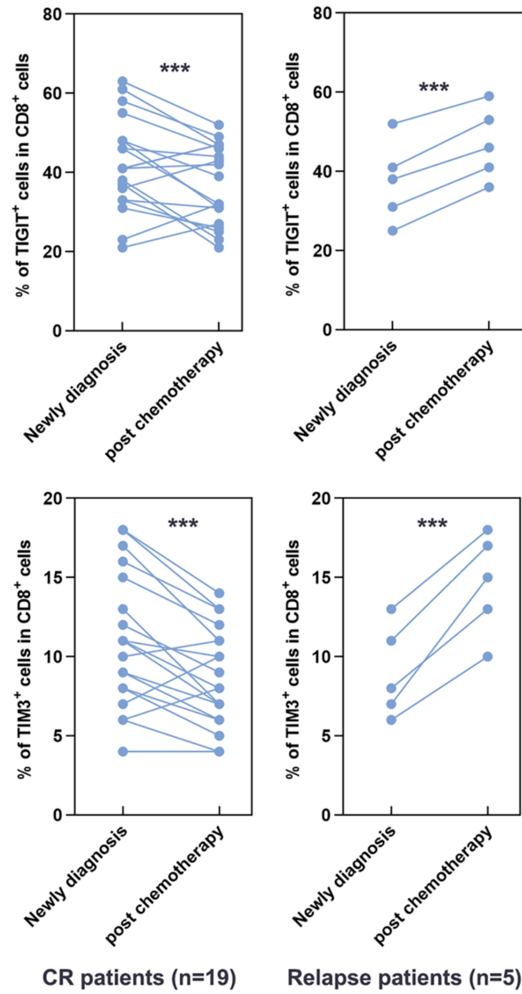

Figure S4. Expression levels of TIGIT and TIM3 in BM $CD8^+$ T cells from patients before and after chemotherapy. Samples collected from patients who relapsed (n = 5) and patients who achieved CR (n = 19) after chemotherapy and analyzed by flow cytometry. The Wilcoxon signed-rank test was used for matched paired comparisons. *** indicates $P < 0.01$.

Table S2. The top 50 clonotypes in CD8+ T cells were frequently distributed in CD8+ PD-1+ populations and CD8+ PD-1- populations

Variable Gene	Diversity Gene	Joining Gene	Constant	CDR3 AA	V Gene Allele	D Gene Allele	J Gene Allele	PD-1+ Freq. (%)	PD-1- Freq. (%)
TRBV6-2	TRBD2	TRBJ2-7	TRBC2	ASSGLAGANDEQY	1	2	1	6.828	0.806
TRBV24-1	TRBD2	TRBJ2-1	TRBC2	ATSAQMDYNEQF	1	1	1	3.252	0.155
TRBV6-2	TRBD2	TRBJ2-1	TRBC2	ASSYKTRRNEQF	1	2	1	2.035	0.000
TRBV7-8		TRBJ2-1	TRBC2	ASSPSPSYNEQF	1		1	3.181	0.069
TRBV4-3	TRBD1	TRBJ2-3	TRBC2	ASSQANQGNTQY	1	1	1	2.150	0.086
TRBV6-2	TRBD2	TRBJ2-5	TRBC2	ATMGLAGVETQY	1	2	1	1.947	0.083
TRBV4-1		TRBJ1-5	TRBC1	ASSQSAVSNQPQH	1		1	3.737	0.056
TRBV19	TRBD1	TRBJ1-2	TRBC1	ASSFGTSDGYT	1	1	1	1.696	0.000
TRBV29-1	TRBD2	TRBJ2-3	TRBC2	SVRTTSTDTQY	1	1	1	1.794	0.413
TRBV19	TRBD1	TRBJ2-1	TRBC2	ASSTYSDSNNEQF	1	1	1	0.856	0.338
TRBV11-2	TRBD1	TRBJ2-7	TRBC2	ASGPGTVFEQY	3	1	1	0.787	0.276
TRBV2	TRBD1	TRBJ2-7	TRBC2	ASKDRGYYEQY	1	1	1	0.456	0.200
TRBV6-2	TRBD1	TRBJ1-5	TRBC1	ASSYSYGTGGTSGQPQH	1	1	1	0.450	0.178
TRBV28		TRBJ2-7	TRBC2	ASTAAYEQY	1		1	0.210	0.000
TRBV4-3	TRBD2	TRBJ2-5	TRBC2	ASSQEPPGSKVETQY	1	2	1	0.402	0.190
TRBV5-1		TRBJ2-7	TRBC2	ASRLPGGNEQY	1		1	0.400	0.011
TRBV15	TRBD2	TRBJ2-3	TRBC2	ATSGTSGTPDTQY	2	2	1	0.998	0.846
TRBV12-4		TRBJ1-5	TRBC1	ASSLGVSNQPQH	1		1	0.880	0.036
TRBV11-2	TRBD1	TRBJ2-3	TRBC2	ASSLEGQNTQY	1	1	1	0.862	0.261
TRBV19		TRBJ1-1	TRBC1	ASSISQDTEAF	1		1	0.761	0.526
TRBV5-1	TRBD1	TRBJ2-3	TRBC2	ASSLEQGARTDTQY	1	1	1	0.850	0.058
TRBV18		TRBJ2-3	TRBC2	ASSVTDTQY	1		1	0.399	0.000
TRBV5-4	TRBD1	TRBJ2-3	TRBC2	ASSPTGQGARDTQY	1	1	1	0.765	0.000
TRBV5-1		TRBJ1-1	TRBC1	ASSLELNTEAF	1		1	0.725	0.448
TRBV12-3	TRBD1	TRBJ1-1	TRBC1	ASSWTGGRAF	1	1	1	0.024	0.000
TRBV24-1	TRBD2	TRBJ2-7	TRBC2	ATSDLLYGEQY	1	2	1	0.023	0.080
TRBV20-1		TRBJ2-1	TRBC2	SARAPAGDEQF	1		1	0.023	0.131
TRBV18	TRBD2	TRBJ2-1	TRBC2	ASSLEGPYNEQF	1	2	1	0.219	1.247
TRBV20-1	TRBD1	TRBJ1-1	TRBC1	SARTGELEAF	1	1	1	0.216	1.140
TRBV20-1	TRBD1	TRBJ1-5	TRBC1	SAPLGGLDSQPQH	1	1	1	0.213	2.109
TRBV27	TRBD2	TRBJ2-1	TRBC2	ASIPTGTSGSLYNEQF	1	2	1	0.208	0.109
TRBV5-1	TRBD2	TRBJ1-1	TRBC1	ASSLEGYTEAF	1	2	1	0.203	0.103
TRBV11-1	TRBD2	TRBJ2-1	TRBC2	ASSLEAGVYNEQF	1	2	1	0.200	0.100
TRBV29-1	TRBD2	TRBJ2-1	TRBC2	SVGGISNEQF	1	1	1	0.195	0.000
TRBV5-8	TRBD2	TRBJ2-5	TRBC2	ASSHPATRYIPETQY	1	1	1	0.193	0.094
TRBV9	TRBD1	TRBJ1-5	TRBC1	ASSPRTGPFNQPQH	1	1	1	0.178	0.092
TRBV7-6	TRBD1	TRBJ2-1	TRBC2	ASSRGDEQF	1	1	1	0.177	0.086
TRBV7-2		TRBJ1-2	TRBC1	ASSLAMAGYT	1		1	0.176	0.000
TRBV7-6		TRBJ2-5	TRBC2	ASSSGETQY	1		1	0.175	0.084
TRBV4-1		TRBJ1-3	TRBC1	ASSQAQISGNTIY	1		1	0.170	0.083
TRBV12-3	TRBD2	TRBJ2-1	TRBC2	ASSSTSGRSEQF	1	2	1	0.200	0.313
TRBV2	TRBD2	TRBJ2-1	TRBC2	AGGTPVVDEQF	1	1	1	0.354	0.060
TRBV20-1		TRBJ1-6	TRBC1	SATDHNSPLH	1		1	0.451	0.178
TRBV6-5	TRBD1	TRBJ1-1	TRBC1	ASSYSRQGVTEAF	1	1	1	0.167	0.000
TRBV3-1	TRBD2	TRBJ1-3	TRBC1	ASGGRLSGNTIY	1	1	1	0.548	0.043
TRBV7-6	TRBD1	TRBJ2-7	TRBC2	ASSFRGTALDEQY	1	1	1	0.277	0.247
TRBV7-3		TRBJ2-7	TRBC2	ATRLASYEQY	1		1	0.125	0.072
TRBV5-4		TRBJ2-1	TRBC2	ASSPGPLYLGEQF	1		1	0.125	0.072
TRBV7-2		TRBJ2-5	TRBC2	ASSFDIEETQY	2		1	0.123	0.071
TRBV3-1	TRBD2	TRBJ2-5	TRBC2	ASSQAGGPEPETQY	1	2	1	0.120	0.204

Samples were collected at new diagnosis from patient (Patient #8) who relapsed post chemotherapy.

Table S3. The top 50 clonotypes in CD8+ T cells were frequently distributed in CD8+ PD-1+ populations and CD8+ PD-1- populations

Variable Gene	Diversity Gene	Joining Gene	Constant	CDR3 AA	V Gene Allele	D Gene Allele	J Gene Allele	PD-1+ Freq. (%)	PD-1- Freq. (%)
TRBV10-3	TRBD1	TRBJ2-3	TRBC2	AIGEVEQGNADTQY	2	1	1	15.324	1.253
TRBV4-1	TRBD2	TRBJ2-1	TRBC2	ASSQTLRGGVNEQF	1	2	1	2.091	0.499
TRBV29-1	TRBD1	TRBJ2-5	TRBC2	SVEDDRGRGETQY	1	1	1	1.140	1.062
TRBV29-1	TRBD1	TRBJ2-5	TRBC2	SVESDRGRGETQY	1	1	1	3.927	0.019
TRBV5-1		TRBJ2-1	TRBC2	ASSLDATALNEQF	1		1	2.890	0.000
TRBV13		TRBJ2-7	TRBC2	ASSLVGYEQY	1		1	1.878	0.036
TRBV6-1	TRBD2	TRBJ1-5	TRBC1	ASSGRAVNQPQH	1	2	1	4.798	0.030
TRBV20-1		TRBJ2-5	TRBC2	SASGWSGETQY	1		1	1.779	0.336
TRBV15	TRBD1	TRBJ2-7	TRBC2	ATSLKGTGEQY	2	1	1	1.138	0.041
TRBV28		TRBJ2-7	TRBC2	ASSLDGYEQY	1		1	0.734	0.111
TRBV30	TRBD2	TRBJ2-7	TRBC2	AWSAGEGYEQY	1	2	1	0.634	0.106
TRBV20-1		TRBJ2-1	TRBC2	SARAPAGDEQF	1		1	0.607	0.105
TRBV6-5	TRBD1	TRBJ1-2	TRBC1	ASSYLGQSFHYGYT	1	1	1	0.020	0.518
TRBV2	TRBD2	TRBJ2-7	TRBC2	ASRRTSSPEQY	1	1	1	0.567	0.311
TRBV6-5	TRBD2	TRBJ2-1	TRBC2	ASSYSPRLAGEQF	1	1	1	0.421	0.111
TRBV7-6	TRBD2	TRBJ2-1	TRBC2	ASSPEGAGNAYNEQF	1	1	1	0.019	0.285
TRBV4-1		TRBJ2-3	TRBC2	ASSQESPHTDTQY	1		1	0.351	0.138
TRBV6-4		TRBJ1-1	TRBC1	ASSESANTEAF	1		1	0.811	0.148
TRBV4-3	TRBD1	TRBJ2-3	TRBC2	ASSQANQGNTQY	1	1	1	0.794	0.000
TRBV20-1	TRBD2	TRBJ2-1	TRBC2	SAATSSGYNEQF	5	1	1	0.680	0.000
TRBV7-9		TRBJ1-1	TRBC1	ASSLLHGKNTEAF	1		1	0.969	0.020
TRBV12-3	TRBD2	TRBJ1-2	TRBC1	ASSLIAGAGYGYT	1	2	1	0.363	0.000
TRBV7-8		TRBJ2-7	TRBC2	ASSLDGPVQY	1		1	1.257	0.021
TRBV20-1		TRBJ2-3	TRBC2	SASHGNSDTQY	5		1	0.143	0.004
TRBV6-5		TRBJ1-5	TRBC1	ASSLKPPGEGQPQH	1		1	0.736	0.011
TRBV7-8		TRBJ2-2	TRBC2	ASSPGELF	1		1	0.227	0.008
TRBV6-1	TRBD1	TRBJ1-5	TRBC1	ASRDWGYPQPQH	1	1	1	0.223	0.058
TRBV13	TRBD2	TRBJ2-7	TRBC2	ASSSHGVSYEQY	1	1	1	0.210	0.122
TRBV4-3	TRBD1	TRBJ2-1	TRBC2	ASSQDAAGQVYNEQF	1	1	1	0.208	3.503
TRBV6-1	TRBD2	TRBJ1-2	TRBC1	ASSDPGGRGYGYT	1	2	1	0.874	2.831
TRBV4-1	TRBD1	TRBJ2-7	TRBC2	ASSQTGQGSSLSYEQY	1	1	1	0.202	0.623
TRBV4-1	TRBD2	TRBJ2-4	TRBC2	ASSQGGRALFAIQY	1	2	1	0.020	0.537
TRBV27	TRBD2	TRBJ2-3	TRBC2	ASSSRLAGGTDTQY	1	2	1	0.118	0.528
TRBV9	TRBD1	TRBJ2-1	TRBC2	ASSPQGSSYNEQF	1	1	1	0.185	0.657
TRBV7-2		TRBJ2-5	TRBC2	ASSDQETQY	1		1	0.180	0.789
TRBV28		TRBJ2-7	TRBC2	ASTAAYEQY	1		1	0.172	0.253
TRBV20-1		TRBJ2-5	TRBC2	SARDGKGSETQY	5		1	0.172	0.253
TRBV4-1		TRBJ2-1	TRBC2	ASSHGRLTDEQF	1		1	0.078	0.384
TRBV27		TRBJ2-2	TRBC2	ASSYGSGELF	1		1	0.071	0.314
TRBV6-2	TRBD1	TRBJ1-5	TRBC1	ASTLDTYSNQPQH	1	1	1	0.018	0.105
TRBV20-1	TRBD1	TRBJ2-1	TRBC2	SAPPRGLGNEQF	1	1	1	0.334	0.072
TRBV20-1	TRBD2	TRBJ1-2	TRBC1	SVVGGAGGYT	5	1	1	0.230	0.024
TRBV4-1	TRBD2	TRBJ2-1	TRBC2	ASSWELGEQF	1	1	1	0.320	0.037
TRBV27	TRBD1	TRBJ2-1	TRBC2	ASSPTPGTGVYNEQF	1	1	1	0.207	0.017
TRBV12-4	TRBD2	TRBJ2-1	TRBC2	ASSFDFYPSGSSGNEQF	1	2	1	0.638	0.010
TRBV10-3	TRBD2	TRBJ1-6	TRBC1	AIRGGDPDSPLH	2	1	1	0.738	0.010
TRBV29-1	TRBD2	TRBJ2-5	TRBC2	SASPGLSGETQY	1	1	1	0.104	0.099
TRBV5-1	TRBD1	TRBJ2-3	TRBC2	ASSLEQGARTDTQY	1	1	1	0.102	0.097
TRBV29-1	TRBD2	TRBJ2-1	TRBC2	SVVPSGRNNEQF	1	2	1	0.099	0.096
TRBV6-2		TRBJ2-3	TRBC2	ASSTSSVDTQY	1		1	0.099	0.094

Samples were collected after treatment from patient (Patient #8) who relapsed post chemotherapy.

Table S4. The top 50 clonotypes in CD8+ T cells were frequently distributed in CD8+ PD-1+ populations and CD8+ PD-1- populations

Variable Gene	Diversity Gene	Joining Gene	Constant	CDR3 AA	V Gene Allele	D Gene Allele	J Gene Allele	PD-1+ Freq. (%)	PD-1- Freq. (%)
TRBV6-6	TRBD1	TRBJ1-1	TRBC1	ASSSSGTGNTEAF	1	1	1	6.013	0.157
TRBV5-1	TRBD1	TRBJ2-7	TRBC2	ASSFETEIDEQY	1	1	1	3.878	0.120
TRBV24-1	TRBD1	TRBJ2-1	TRBC2	ATSEGDSYNEQF	1	1	1	1.684	0.367
TRBV11-1	TRBD1	TRBJ2-7	TRBC2	ASSLEGPTYEQY	1	1	1	2.667	0.098
TRBV11-2	TRBD1	TRBJ2-5	TRBC2	ASSSGQVQETQY	1	1	1	2.519	0.029
TRBV20-1	TRBD1	TRBJ1-2	TRBC1	SARGLTVADGYT	5	1	1	3.390	0.257
TRBV9		TRBJ1-6	TRBC1	ASSGPNSPLH	1		1	1.691	1.676
TRBV9	TRBD2	TRBJ1-2	TRBC1	ASSGKPGTPHYGYT	1	2	1	1.661	0.059
TRBV7-2	TRBD2	TRBJ2-5	TRBC2	ASSSLGGFQETQY	1	2	1	2.638	0.050
TRBV28	TRBD1	TRBJ2-1	TRBC2	ASSYRLLSNNEQF	1	1	1	0.624	0.049
TRBV27		TRBJ1-5	TRBC1	ASSLDVRSNQPQH	1		1	0.589	0.048
TRBV28	TRBD2	TRBJ2-1	TRBC2	ASTLTSGSTDEQF	1	2	1	0.536	0.042
TRBV7-2	TRBD1	TRBJ2-5	TRBC2	ASSLAPGLDEKTQY	1	1	1	0.533	0.041
TRBV14	TRBD2	TRBJ2-7	TRBC2	ASSLLAENEQY	2	1	1	0.474	0.040
TRBV6-6		TRBJ2-1	TRBC2	ASSYIQVGEQF	1		1	0.452	0.393
TRBV20-1		TRBJ2-7	TRBC2	SARTTESYEQY	5		1	0.020	0.367
TRBV12-4		TRBJ2-7	TRBC2	ASSLNGYVHEQY	1		1	0.403	0.035
TRBV27	TRBD2	TRBJ2-1	TRBC2	ASSTLPSGNNEQF	1	2	1	0.598	0.024
TRBV9	TRBD2	TRBJ2-2	TRBC2	ASSGSRLAGGKHAGELF	1	2	1	0.564	0.260
TRBV13		TRBJ1-1	TRBC1	ASSLADMNTEAF	1		1	0.764	0.000
TRBV10-3	TRBD2	TRBJ1-4	TRBC1	AISGGPGEKLF	3	1	1	0.897	0.000
TRBV28	TRBD2	TRBJ2-3	TRBC2	ASSYHWSGAGVTDTQY	1	2	1	0.358	0.474
TRBV4-1	TRBD2	TRBJ2-7	TRBC2	ASSQEFGLAGGAYEQY	1	2	1	0.345	0.049
TRBV14	TRBD1	TRBJ1-5	TRBC1	ASSQDRTGPRH	2	1	1	0.080	0.000
TRBV7-2		TRBJ1-5	TRBC1	ASSLFPETVTRQPQH	2		1	0.127	0.036
TRBV7-6	TRBD1	TRBJ1-2	TRBC1	ASSMTGLYGYT	1	1	1	0.023	0.259
TRBV12-4		TRBJ2-3	TRBC2	ASSLDTQY	1		1	0.225	0.248
TRBV7-2	TRBD1	TRBJ1-1	TRBC1	ASSLVQGNTEAF	2	1	1	0.022	0.227
TRBV4-1	TRBD1	TRBJ2-5	TRBC2	ASSQSGTSQETQY	1	1	1	0.022	0.225
TRBV6-2	TRBD2	TRBJ2-1	TRBC2	ASTPPGLAGGRGEQF	1	2	1	0.208	0.139
TRBV18	TRBD2	TRBJ2-7	TRBC2	ASSPPSSGGGREQY	1	2	1	0.208	0.138
TRBV16	TRBD1	TRBJ1-2	TRBC1	ASSHRTGGFYGYT	1	1	1	0.201	0.133
TRBV20-1	TRBD1	TRBJ2-7	TRBC2	SARDPGQGSYEQY	5	1	1	0.192	0.210
TRBV5-6	TRBD1	TRBJ1-2	TRBC1	ASSLTGVHGYT	1	1	1	0.185	0.089
TRBV5-4		TRBJ2-1	TRBC2	ASSLESVWSYNEQF	1		1	0.174	0.089
TRBV6-1	TRBD1	TRBJ2-2	TRBC2	ASQFQGRITGELF	1	1	1	0.173	0.172
TRBV19		TRBJ1-1	TRBC1	ASSIRYTEAF	1		1	0.172	0.113
TRBV28	TRBD1	TRBJ1-6	TRBC1	ASDSLSTGYNSPLH	1	1	1	0.162	0.162
TRBV9		TRBJ1-6	TRBC1	ASSGSNSPLH	1		1	0.160	0.101
TRBV7-2	TRBD2	TRBJ2-7	TRBC2	ASSPTSGSSYEQY	1	1	1	0.157	0.098
TRBV14	TRBD2	TRBJ2-1	TRBC2	ASSLTPGSEQF	2	2	1	0.855	0.000
TRBV9	TRBD2	TRBJ2-2	TRBC2	ASSGPTSGRAHTGELF	1	2	1	0.744	0.194
TRBV30	TRBD2	TRBJ2-1	TRBC2	AWTLAGDYNEQF	1	2	1	0.738	0.050
TRBV29-1	TRBD1	TRBJ2-1	TRBC2	SVEQALGDRVNEQF	1	1	1	0.590	0.000
TRBV9	TRBD2	TRBJ2-7	TRBC2	ASSPPGLGYEQY	1	1	1	0.627	0.091
TRBV29-1		TRBJ2-3	TRBC2	SVEFGDTQY	1		1	0.942	0.000
TRBV7-2		TRBJ2-7	TRBC2	ASSSGLGTYEQY	1		1	0.764	0.142
TRBV6-1	TRBD2	TRBJ2-5	TRBC2	ASSQGLDLETQY	1	1	1	0.622	0.134
TRBV20-1	TRBD2	TRBJ2-2	TRBC2	SASSGREFGELF	1	2	1	0.895	0.130
TRBV20-1	TRBD2	TRBJ2-3	TRBC2	SASPSRGPSGISDTQY	5	2	1	0.418	0.129

Samples were collected at new diagnosis from patient (Patient #19) with sustained CR post chemotherapy.

Table S5. The top 50 clonotypes in CD8+ T cells were frequently distributed in CD8+ PD-1+ populations and CD8+ PD-1- populations

Variable Gene	Diversity Gene	Joining Gene	Constant	CDR3 AA	V Gene Allele	D Gene Allele	J Gene Allele	PD-1+ Freq. (%)	PD-1- Freq. (%)
TRBV29-1	TRBD1	TRBJ2-3	TRBC2	SVEWGREGASTDTQY	1	1	1	8.169	0.734
TRBV29-1	TRBD2	TRBJ2-1	TRBC2	SVPQTLSSGPEHEQF	1	1	1	2.272	0.362
TRBV28	TRBD1	TRBJ2-3	TRBC2	ASSRDGRTDTQY	1	1	1	0.910	0.131
TRBV5-6	TRBD1	TRBJ2-3	TRBC2	ASSLAPTGSTDTQY	1	1	1	1.742	0.000
TRBV3-1	TRBD2	TRBJ2-1	TRBC2	ASSQGRDYPYNEQF	1	1	1	1.736	0.172
TRBV14	TRBD2	TRBJ2-7	TRBC2	ASSREYEQY	1	2	1	1.772	0.000
TRBV28	TRBD1	TRBJ1-1	TRBC1	ASSLPGQNTEAF	1	1	1	1.419	0.098
TRBV28	TRBD1	TRBJ1-5	TRBC1	ASSRGQPQH	1	1	1	1.417	0.061
TRBV7-2	TRBD2	TRBJ2-7	TRBC2	ASSFSGLGYEQY	1	1	1	1.399	0.056
TRBV2	TRBD1	TRBJ2-1	TRBC2	ASSRGGAVDEQF	1	1	1	0.335	0.050
TRBV9	TRBD2	TRBJ2-5	TRBC2	ASSPEETSGQETQY	1	1	1	0.589	0.048
TRBV30	TRBD2	TRBJ2-1	TRBC2	AWTLAGDYNEQF	1	2	1	0.670	0.043
TRBV9	TRBD2	TRBJ2-1	TRBC2	ASSVGTFNEQF	1	1	1	0.276	0.043
TRBV29-1		TRBJ2-7	TRBC2	SVELYRVGQYVNEQY	1		1	0.874	0.043
TRBV29-1		TRBJ1-1	TRBC1	SVAPVNTEAF	1		1	0.226	0.042
TRBV29-1		TRBJ1-1	TRBC1	SVETTQNTEAF	1		1	0.226	0.000
TRBV20-1	TRBD2	TRBJ2-2	TRBC2	SASSGREFGELF	1	2	1	0.207	0.038
TRBV23-1	TRBD1	TRBJ2-5	TRBC2	ASSARGLTQETQY	1	1	1	0.896	0.031
TRBV4-3	TRBD2	TRBJ2-5	TRBC2	ASSYGTAGAQY	1	1	1	0.695	0.030
TRBV29-1		TRBJ2-1	TRBC2	SVEEPRSNEQF	1		1	0.781	0.030
TRBV29-1	TRBD1	TRBJ2-5	TRBC2	SVGGHKETQY	1	1	1	0.679	0.000
TRBV6-2		TRBJ2-5	TRBC2	ASSSSQETQY	1		1	0.578	0.029
TRBV7-2	TRBD2	TRBJ2-5	TRBC2	ASSSLGGFQETQY	1	2	1	0.876	0.029
TRBV5-6		TRBJ2-7	TRBC2	ASSLDRSYEQY	1		1	0.466	0.018
TRBV6-2	TRBD2	TRBJ2-5	TRBC2	ASSYPGIRDSIVLQETQY	1	2	1	0.963	0.000
TRBV14	TRBD1	TRBJ1-2	TRBC1	ASRGQLTDGYT	1	1	1	0.137	0.017
TRBV29-1	TRBD2	TRBJ2-3	TRBC2	SVEDEVAGVFSTDTQY	1	1	1	0.137	0.016
TRBV12-4		TRBJ2-7	TRBC2	ASSLNGYVHEQY	1		1	0.135	0.000
TRBV7-6	TRBD2	TRBJ2-3	TRBC2	ASTPNQRGVTDTQY	1	1	1	0.108	1.160
TRBV11-3	TRBD2	TRBJ2-1	TRBC2	ASSLLAGDNEQF	1	1	1	0.107	1.154
TRBV5-4	TRBD1	TRBJ1-2	TRBC1	ASSLLGDDGYT	1	1	1	0.020	0.878
TRBV14		TRBJ2-1	TRBC2	ASSLTHNEQF	1		1	0.073	0.605
TRBV29-1		TRBJ2-3	TRBC2	SVGGKLLTDTQY	1		1	0.064	0.417
TRBV14	TRBD1	TRBJ1-2	TRBC1	ASSQGPGQEGFNYGYT	1	1	1	0.089	0.482
TRBV14		TRBJ2-2	TRBC2	ASSPIVFDGELF	2		1	0.087	0.206
TRBV29-1	TRBD2	TRBJ2-7	TRBC2	SVGLADAYEQY	1	1	1	0.041	0.197
TRBV29-1	TRBD1	TRBJ2-3	TRBC2	SVSSLQKQGTQY	1	1	1	0.031	0.190
TRBV29-1	TRBD2	TRBJ2-3	TRBC2	SVRLAGGPGTQY	1	2	1	0.020	0.168
TRBV7-2	TRBD2	TRBJ2-2	TRBC2	ASSLLPQLAGGPSDGELF	1	2	1	0.083	0.165
TRBV29-1	TRBD1	TRBJ1-4	TRBC1	SAAGHLNEKLF	1	1	1	0.028	0.165
TRBV28	TRBD1	TRBJ1-1	TRBC1	ASSFQGTEAF	1	1	1	0.973	0.000
TRBV18	TRBD2	TRBJ2-7	TRBC2	ASSPPSSGGGREQY	1	2	1	0.771	0.159
TRBV2	TRBD1	TRBJ1-1	TRBC1	ARGDRDTEAF	1	1	1	0.978	0.156
TRBV23-1	TRBD2	TRBJ2-7	TRBC2	ASSQPRGGQRYEQY	1	2	1	0.477	0.000
TRBV23-1	TRBD2	TRBJ2-1	TRBC2	ASSHLTSGGSYNEQF	1	1	1	0.477	0.000
TRBV28	TRBD2	TRBJ2-7	TRBC2	ASTIKGSTPYEQY	1	2	1	0.367	0.148
TRBV28	TRBD2	TRBJ2-3	TRBC2	ASSYHWSGAGVTDTQY	1	2	1	0.199	0.147
TRBV14	TRBD2	TRBJ2-1	TRBC2	ASSRLAGGPIDEQF	1	1	1	0.074	0.145
TRBV7-9	TRBD2	TRBJ2-4	TRBC2	ASSPLMTGGNIQY	1	2	1	0.164	0.136
TRBV7-2	TRBD2	TRBJ2-2	TRBC2	ASSLDNSVRTGELF	1	1	1	0.255	0.129

Samples were collected after treatment from patient (Patient #19) with sustained CR post chemotherapy.

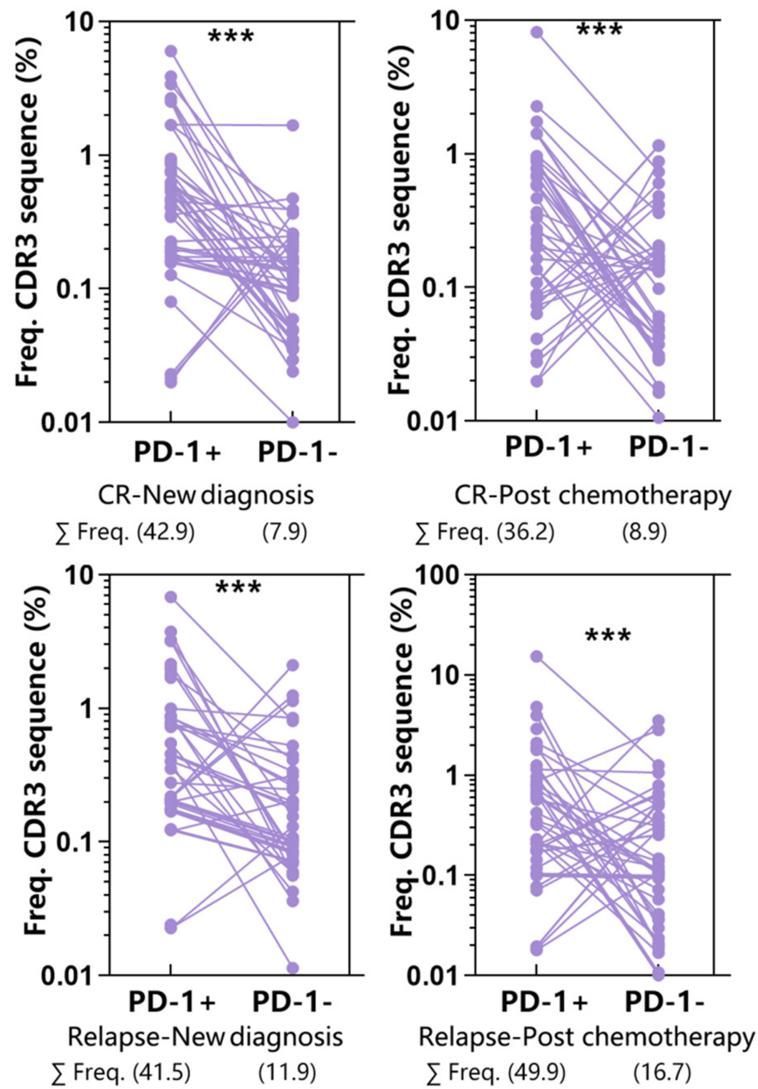

Figure S5. The top 50 clonotypes in $CD8^+$ PD-1^+ T cells were frequently distributed in $CD8^+$ PD-1^- populations. A dot is used to represent one patient or one donor sample. CR: patients who were newly diagnosed with AML and remained in complete remission after chemotherapy. Relapse: patients who were newly diagnosed with AML and relapsed post chemotherapy. The Wilcoxon signed-rank test was used for matched paired comparisons. *** indicates $P < 0.01$.